DFT MODELING OF CO_2 CAPTURE MECHANISM OVER (N-METHYLAMINOPROPYL)-TRIMETHOXYSILANE-MODIFIED MESOPOROUS SILICA

by

Kıvanç Başaran

Submitted to Graduate School of Natural and Applied Sciences
in Partial Fulfillment of the Requirements
for the Degree of Master of Science in
Chemical Engineering

Yeditepe University

2022

DFT MODELING OF CO_2 CAPTURE MECHANISM OVER (N-METHYLAMINOPROPYL)-TRIMETHOXYSILANE-MODIFIED MESOPOROUS SILICA

APPROVED BY:

Prof. Dr. Tuğba Davran-Candan ……
(Thesis Supervisor)
(Yeditepe University)

Prof. Dr. Nihan Çelebi-Ölçüm ……
(Yeditepe University)

Assist. Prof. Dr. Oluş Özbek ……
(Gebze Technical University)

DATE OF APPROVAL: …./…./2022

I hereby declare that this thesis is my own work and that all information in this thesis has been obtained and presented in accordance with academic rules and ethical conduct. I have fully cited and referenced all material and results as required by these rules and conduct, and this thesis study does not contain any plagiarism. If any material used in the thesis requires copyright, the necessary permissions have been obtained. No material from this thesis has been used for the award of another degree.

I accept all kinds of legal liability that may arise in case contrary to these situations.

Name, Last name ……

Signature …..…….……..

ACKNOWLEDGEMENTS

Firstly, I would like to thank my thesis advisor Prof. Tuğba Davran-Candan for her technical and emotional support during this project. Her guidance guided me in researching and writing this thesis.

In addition, my best friend and wife Sinem Hassan Başaran, who has always been by my side and my parents for making me feel that they have always supported me throughout my life.

I would like to thank my friends, Egemen Havuz, Katia Haviters, Berk Alarcin, Ezgi Uslu, Beril Gülkaya, Nur Çınar, Kemal Düzkar, Beyza Abişoğlu, Barış Emek, Avram Aruh, Nermin Şen, Yeşim Çamlısoy, Sezen Alsancak with whom we walked on the graduate journey and worked for the Department of Chemical Engineering at Yeditepe University.

Yeditepe University financed this research as part of the YAP (Yeditepe University Research Projects and Scientific Activities) program with the project number YAP-LP-FEB-19007.

ABSTRACT

DFT MODELING OF CO_2 CAPTURE MECHANISM OVER (N-METHYLAMINOPROPYL)-TRIMETHOXYSILANE-MODIFIED MESOPOROUS SILICA

Determination of the CO_2 interaction mechanisms with amine-modified solid adsorbents plays an important role in the development of highly efficient sorbents that would meet the future requirements to mitigate the severe effects of global warming. Accordingly, this study aimed to examine the CO_2 capture mechanism over trimethoxy[3-(methylamino)propyl]silane (MAPS)-functionalized mesoporous silica using DFT modeling and to clarify the effect of free surface silanol density as well as amine density on the capture mechanism. Our calculations indicated that carbamic acid and ammonium carbamate were the two main products, formation of both requiring amine pairs rather than isolated amine structures. Besides, surface silanols were observed to play a significant role on the capture of CO_2, they were not only effective on the stabilization of the adsorption species but can also directly participate in the reaction mechanism. Amine functionality, on the other hand, seemed to be less deterministic on the capture under the conditions employed in this study.

ÖZET

(N-METİLAMİNOPROPİL)-TRİMETOKSİSİLAN İLE MODİFİYE EDİLMİŞ MEZOPORLU SİLİKA ADSORBANLARI ÜZERİNDE CO_2 TUTUNMA MEKANİZMASININ DFT KULLANILARAK MODELLENMESİ

Karbondioksitin amin ile modifiye edilmiş katı adsorbanlar ile olan etkileşim mekanizmalarının belirlenmesi, küresel ısınmanın zararlı etkilerini hafifletmek için gelecekte kullanılacak olan yüksek performanslı sorbentlerin geliştirilmesinde önemli bir rol oynamaktadır. Bu nedenle, bu çalışma karbon dioksitin DFT modellemesi kullanılarak trimetoksi[3-(metilamino)propil]silan (MAPS) ile modifiye edilmiş mezeporlu silika adsorbanları üzerindeki tutulum mekanizmalarının incelenmesini ve yüzeyde bulunan serbest silanol yoğunluğu ile birlikte amin yoğunluğunun bu mekanizmalar üzerindeki etkilerini incelemeyi amaçlamaktadır. Yaptığımız hesaplamalar karbon dioksitin amonyum karbamat ve karbamik asit olarak tutulduğunu, her iki yapının oluşumu için izole amin yapılarından ziyade amin çiftlerine ihtiyaç duyulduğunu göstermiştir. Ayrıca, yüzey silanollerinin karbon dioksitin tutunumunda önemli bir rol oynadığı gözlemlenmiş, bu rolün sadece adsorpsiyon sırasında oluşan yapıların stabilizasyonuyla sınırlı kalmadığı, bu yapıların reaksiyon mekanizmasına doğrudan katılabildikleri de görülmüştür. Diğer yandan, bu çalışmada kullanılan koşullar altında amin türünün karbon dioksit yakalama mekanizmaları üzerinde belirleyici bir etkisi olmadığı da gözlenmiştir.

TABLE OF CONTENTS

LIST OF FIGURES

LIST OF SYMBOLS/ABBREVIATIONS

AEAPS	[N(2-aminoethyl)-3aminopropyl]trimethoxysilane
AMP	2amino-2-methyl-1-propanol
APMDES	3-aminopropyl-methyldiethoxysilane
APTMS	3-aminopropyl-triethoxysilane
B3LYP	Becke's three parameter hybrid functional
CCS	Carbon capture and storage
DEA	Diethanolamine
DFT	Density Functional Theory
DMAPS	[3-(diethylamino)propyl]trimethoxysilane
E	Electronic energy
E_j	Exchange energy
E_T	Kinetic energy
E_V	Potential energy
E_{XC}	Exchange-correlation functionals
$\hat{H}$	Hamiltonian operator
FTIR	Fourier transform infrared spectrophotometer
GGA	Generalized gradient approximation
GHG	global greenhouse gas
LDA	Local density approximation
MAPS	Trimethoxy[3-(methylamino)propyl]silane
MEA	Monoethanolamine

MCM-41	Mobile Composition Matter No41
MDEA	Methyldiethanolamine
MOF	Metal organic frameworks
NMR	Nuclear magnetic resonance
PEI	Polyethyleneimine
SBA-15	Santa Barbara Amorphous type material
STQN	Synchronous Transit-Guided Quasi-Newton
TEPA	Tetraethylenepentamine
TS	Transition state
Ψ	Wave function

1. INTRODUCTION

Rapid increase of carbon dioxide (CO_2) levels in the atmosphere, which has started with the industrialization and is gaining momentum at last decades, has been found guilty of causing global warming which is the most highlighted environmental problem of the century. Capture of CO_2 from large-point sources and subsequent sequestration of the gas in proper geological formations (which is known as CCS) has been proposed as one of the most viable near-term solutions to cope with the enormously-increasing atmospheric CO_2 levels [1].

The most conventional way of removing CO_2 from flue gases is absorption which is achieved by liquid amine solutions. Despite of the well-known mechanism of absorption and high CO_2 uptakes of liquid amines, this method is still too expensive for use in industrial scale mainly due to its energy-intensive nature. Thus, it is important to develop alternative ways for the capture of CO_2 that would overcome the problems inherited in aqueous amine absorption [2].

Amine-modified solid adsorbents have emerged as potential alternatives combining the advantage of low regeneration energies of solid sorbents with the high affinity of amines towards CO_2. Tremendous amount of research has been implemented in the field, most of them focusing on the measurement of adsorption capacities of the developed sorbents using various amine structures [3-5], mechanistic studies concentrating of the determination of the adsorption mechanisms being still very few. However, it is quite clear that rational design is required for the development of a highly-efficient adsorbent that would restrict the CO_2 emissions and a solid knowledge of adsorption mechanisms is indispensable for this [6].

Accordingly, this study involves the theoretical investigation of CO_2 adsorption over trimethoxy[3-(methylamino)propyl]silane (MAPS) - modified mesoporous silica with the aim of elucidating the adsorption mechanisms as well as the potential effect of surface silanols and surface amine density on the reaction mechanisms. For this, two different mesoporous silica models resulting in two distinct amine densities and surface silanol densities were used.

Chapter 2 includes the theoretical background and literature survey on the CO_2 capture over amine-modified sorbents whereas Chapter 3 includes computational models, parameters and

methodology. In Chapter 4, obtained results are presented and discussed and finally, the basic conclusions and recommendations for future studies are summarized in Chapter 5.

2. THEORETICAL BACKGROUND

2.1. CO_2 CAPTURE

Global warming, being responsible for the climate change, has been one of the most alarming issues on Earth in the last few decades. CO_2 is the most considerable greenhouse gas that constitutes 65 percent of the global greenhouse gas (GHG) emissions caused mainly by the combustion of fossil fuels [7-9]. According to the information given by the Environmental Protection Agency of the United States, the contribution of the electricity and heat production to the global GHG emissions is the largest (25 percent) and is followed by that of the forestry, agriculture and other land use (24 percent), transportation (14 percent), buildings (6 percent), industry (21 percent), and other (10 percent) [10]. It is predicted that the atmospheric concentration of CO_2 will reach 1360 ppm by the year 2100 without the issue of any climate policies and this will result in a temperature increase of 1.9 to 3.5°C in the atmosphere [11]. Hence, it is necessary to cut down the anthropogenic emissions immediately. More than 190 countries have signed contracts to reduce the GHG emissions to avoid the severe effects of climate change, and keep the global temperature rise below 2°C. Hansen et al. [12] indeed suggested that reducing the CO_2 concentration down to 350 ppm might be necessary to completely prevent or lower the impact of climate change.

Carbon capture and storage (CCS), which involves the capture of CO_2 from large emission sources followed by the transportation and long-term storage of the captured gas in proper geological formations, is one of the most viable ways to achieve this reduction. Of the three steps mentioned above, capture step is the most challenging one requiring the development of cost-effective technologies. There are mainly three developed methods to be utilized in CCS technologies, namely oxy-fuel combustion, pre-combustion, and post-combustion. Oxy-fuel and post combustion can be used in conventional gas and coal plants, while pre-combustion is suitable for integrated gasification combined cycle plants. Pre-combustion method includes the partial oxidation of fuel under air and steam to produce syngas that comprises mainly hydrogen (H_2) and carbon monoxide (CO). Then, CO is reacted with steam (water gas shift reaction) to form more H_2 and CO_2, which is followed by the separation of the obtained CO_2 from the high purity H_2 stream [13]. In oxy-fuel combustion, air is separated into O_2 and N_2 using air separators and combustion is achieved under pure oxygen

resulting H_2O and CO_2 which is easy to separate [14]. Finally, CO_2 is separated from the flue gas obtained from combustion of fuels in post combustion capture [15]. Despite of the ease of CO_2 separation in case of oxy-fuel combustion and pre-combustion approaches, post-combustion technique is the most widely used approach due to its compatibility with the existing systems.

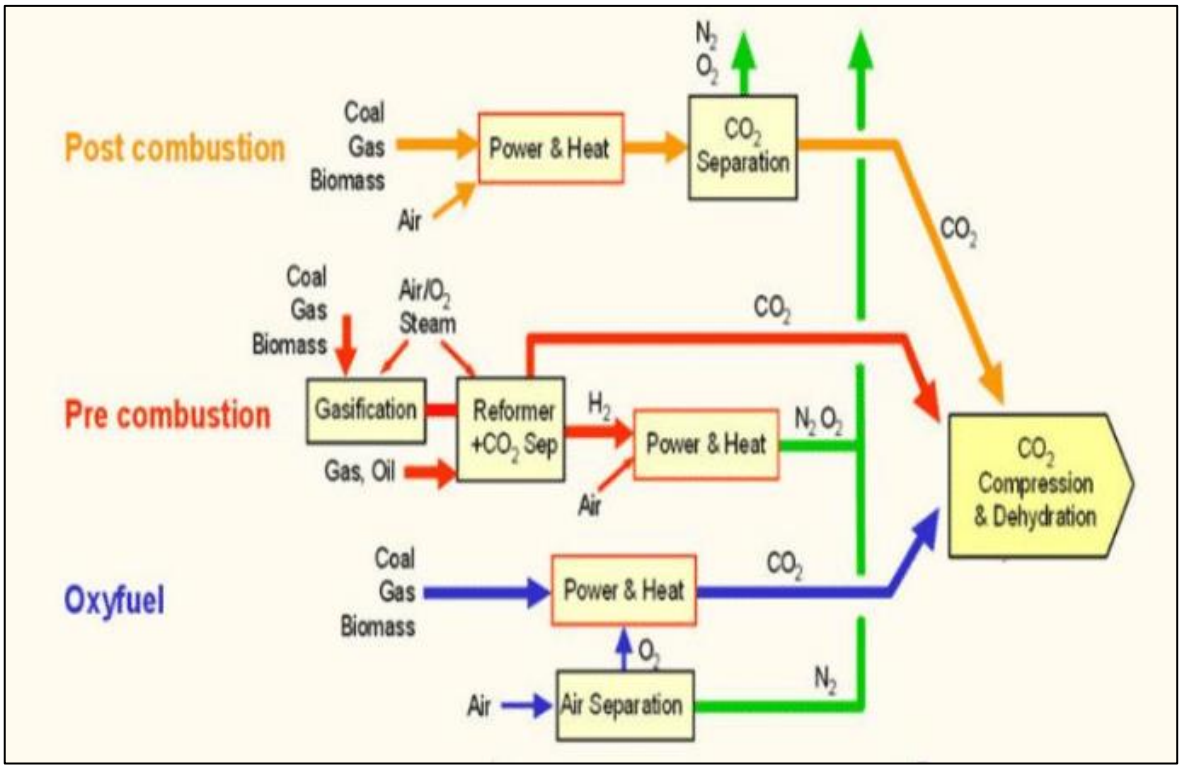

Figure 2.1. CCS Technologies [16]

Liquid amine absorption is the most conventional method that is used in post-combustion capture. Although many different types of amines have been investigated, monoethanolamine (MEA) is the most frequently studied one forming the building blocks of research area as well as the pioneering predictions and further research on other amines. MEA, being a primary amine, interacts quite strongly with CO_2 even under low partial pressures; which in turn makes the CO_2 capture by MEA quite effective and fast under the flue gas conditions. This strong interaction, however, results in extremely high regeneration energies (up to 70 percent of CO_2 capture plant's operating costs) preventing this technology to be used in large scale. Solvent degradation as well as corrosivity were also reported to be serious problems associated with this system [17-19]. To overcome these drawbacks, a wide

variety of different alkanolamine structures have been examined involving diethanolamine(DEA) as a secondary amine, and methyldiethanolamine(MDEA) as a tertiary amine and various blends of these structures. When regeneration energies were investigated, they were found to follow the order MEA > DEA > MDEA [20]. MDEA, being a tertiary amine, had the lowest regeneration energy but its absorption capacity was reported to be quite poor due to the slow reaction kinetics of tertiary amines with CO2 [21,22]. 2amino-2-methyl-1-propanol (AMP), a sterically hindered amine, was also studied thoroughly because of its low regeneration energy and high equilibrium capacity but its slow reaction kinetics compared to MEA made AMP structure also unsuitable for CO_2 adsorption processes [23,24]. Finally, no single amine structure was found to be preferable over MEA among the studied ones, as each had advantages but also disadvantages.

Despite the fact that there has been a large number of studies in the topic of aqueous amine absorption, this method still requires high cost for industrial use due to the high regeneration costs, solvent degradation and corrosivity. Hence, it is quite clear that other methods that would overcome these shortcomings are required and use of solid adsorbents has emerged as a promising alternative.

2.2. CO_2 ADSORPTION

High regeneration costs linked to the aqueous amine absorption systems are originating from the energy required to heat water. Besides, presence of water induces corrosion in the absorption equipment. Consequently, the idea of using solid sorbents for the capture of CO_2 has been considered as a viable substitute that would eliminate the presence of water as well as the problems related to it and many studies have been performed in this field. Both physical and chemical adsorbents are examined and a minimum adsorption capacity of 2-3 mmol/g sorbent was reported to be necessary to compete with the wet scrubbing systems [25].

2.2.1. Physical Adsorbents

Physical adsorption (physisorption) is an exothermic process including the capture of atoms, molecules, or ions in the vicinity of a solid surface through physical interactions.

Physisorption of CO_2 was achieved by using highly porous adsorbents like activated carbons, zeolites, metal organic frameworks (MOFs), and mesoporous silica [26].

Inorganic carbons could be used in many different forms, like graphene, activated carbon, and carbon nanotubes. Activated carbon is the most commonly used one in the industry for applications as water treatment, gas purification, and etc. because of easy accessibility and low cost. Activated carbon was used for CO_2 adsorption too and performance studies were carried out for different pressure, humidity and temperature conditions.

CO_2 uptake measurements of activated carbon shows a decreasing trend with temperature increase because of the exothermic nature of CO_2 adsorption [27-29]. In contrast to the temperature, the carbon dioxide adsorption capacity of activated carbon increases with increasing pressure [30-32]. It is reported that humidity has a negative effect on activated carbon and zeolites [33].

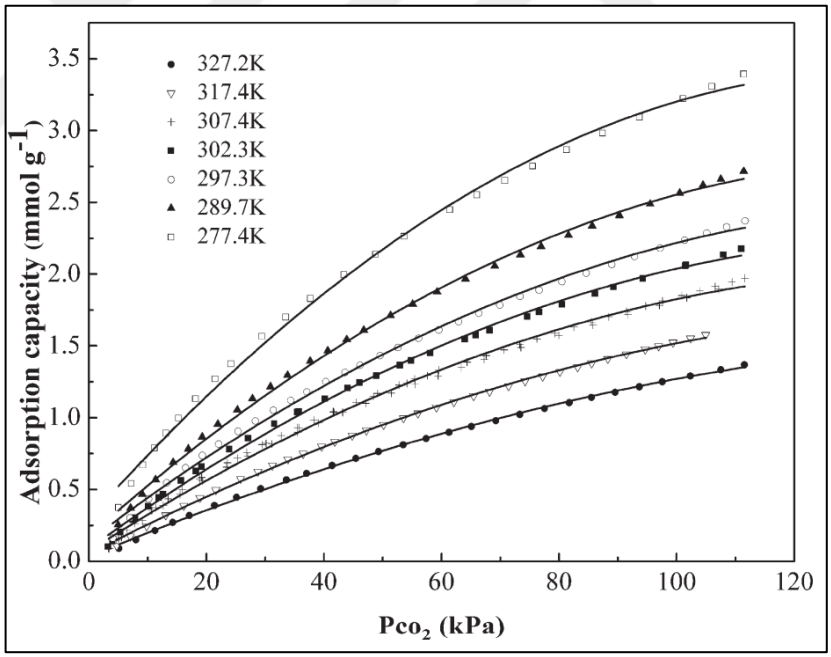

Figure 2.2. CO_2 adsorption capacities of activated carbon for different temperature and pressures [28,29]

Zeolites, with their tunable pore structures, fast reaction kinetics, high stability for adsorption and easy regeneration with high capacity, are the most widely investigated solid sorbents after the activated carbons [29]. Their pore size changes between 0.5 nm to 1.2 nm that

allows to isolate molecules like molecular sieving effect. Previous findings demonstrated that zeolite structures were promising at high pressure and low temperature during dry CO_2 adsorption but lose performance in terms of selectivity, capacity and stability in flue gas conditions [29,32-34].

MOFs, on the other hand, are obtained by combining metal ions or clusters with organic ligands and have crystalline and porous structures. These solid sorbents can be classified as being relatively new compared to zeolites and activated carbons; and have a high potential to be used for CO_2 adsorption due to the fact that they can be easily modified by differentiating the metallic species or the organic linkers which in turn allows the control of pore size, pore shape, chemical potential, selectivity, kinetics and capacity. However, same as with zeolites and activated carbon, they are successful in capturing CO_2 at high pressures and low temperatures. CO_2/H_2O selectivity for MOFs are also very low in humid conditions [33,35,36].

As it is clear from the discussion above, despite of their high performance at high CO_2 partial pressures and low temperature, investigated physical adsorbents are still far from reaching the reported adsorption selectivity and capacity to compete with the aqueous amine systems under the flue gas conditions which is 0.1 bar CO_2 partial pressure and approximately 75°C due to their limited interaction with CO_2. Accordingly, these physical adsorbents were modified with various amine structures in order to benefit from the strong interaction of amines with CO_2 and in this way amine-functionalized solid sorbents have come into play in the search for an effective sorbent for CO_2 capture.

2.2.2. Chemical Adsorbents

Amine-functionalized chemical sorbents are created thorough the surface modification of various physical adsorbents by amine structures; and mesoporous silica, with high surface area, well-arranged pore structures, and large pore diameters, is one of the most widely investigated sorbent for this purpose [37]. Santa Barbara Amorphous type material(SBA-15) and Mobile Composition Matter No 41(MCM-41) are the two well-known types of mesoporous silica structures Both structures contain amorphous pore walls and two-dimensional hexagonal pore configurations. MCM-41 is an organized mesoporous material with a matrix of amorphous silica and homogeneous mesopores. It is the most widely

investigated one over the several mesoporous silicas due to its structural simplicity and ease of fabrication with minimal pore networking and pore-blocking. Tunable pore diameters between 1.5 and 10 nm, enormous pore volumes more than 0.6 cm^3/g, and a very high surface area ranging between 700-1500 m^2/g are the most significant aspects of MCM-41 (Figure 2.3). SBA-15 was, on the other hand, synthesized using silica nanoparticles with substantially wider pores ranging in size from 4.6 to 30 nm. Because of its tunable pores and robust pore walls, SBA-15 is also one of the most studied mesoporous silica structures [33,38].

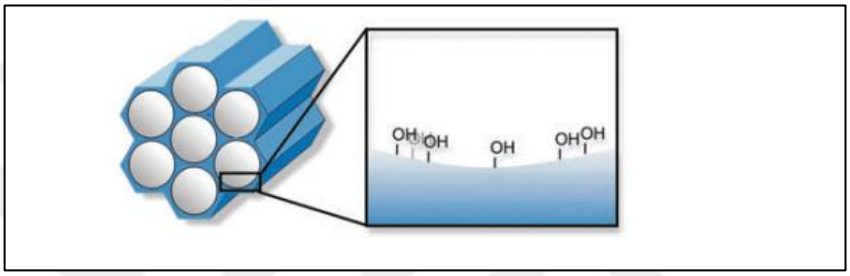

Figure 2.3. Mesoporous silica structure [39]

Grafting and impregnation are the most frequently used techniques for the surface modification of mesoporous silica. In the impregnation process, surface functionalization takes place through the weak van der Waals interactions after the amine-containing solution contacts the sorbent. Amine loading is usually high and the degree of loading is proportional to the pore size of the mesoporous silica. In grafting, on the other hand, surface is modified through a condensation reaction taking place between the $–OCH_3$ groups of the organosilane molecule and the surface silanols of the mesoporous silica. The schematic representation of grafting is given in Figure 2.4.

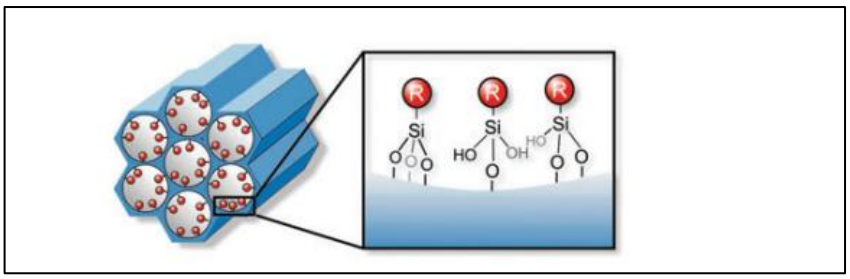

Figure 2.4. R-Grafted meseporous silica structure [39]

Amine loading is usually lower compared to that of the impregnated samples and the degree of loading is limited by the surface silanol density of the mesoporous silica. Figures 2.5 and 2.6 presents the structures of various aminosilane molecules used for surface modification [14,36].

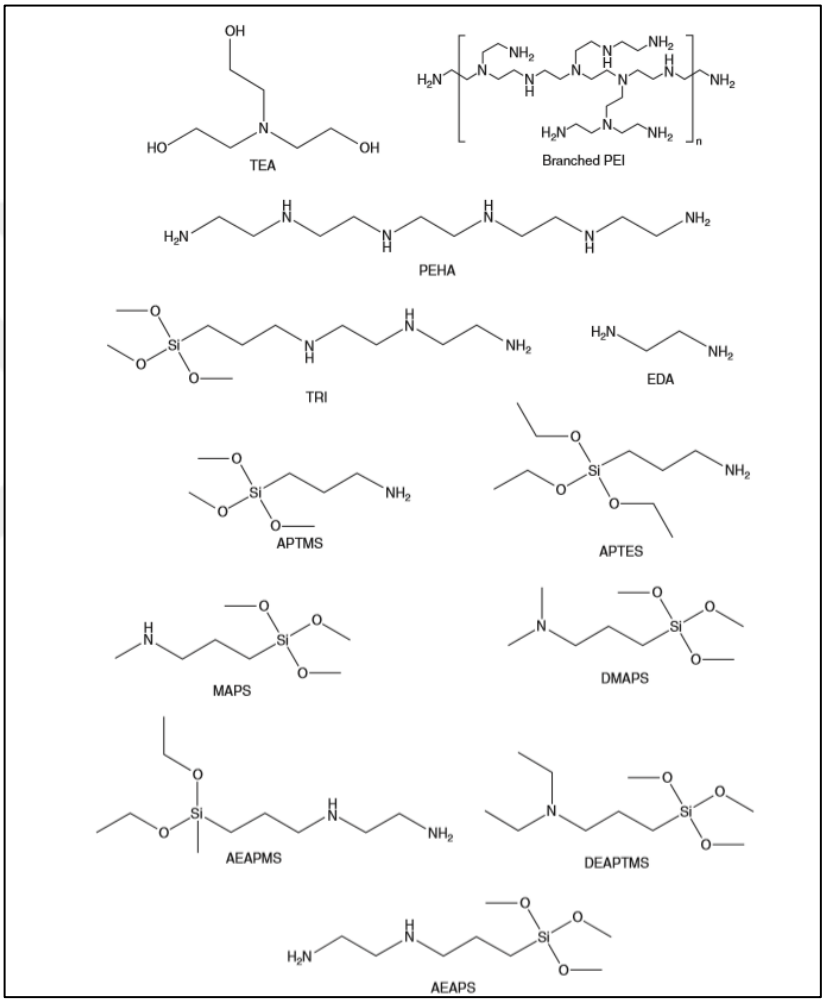

Figure 2.5. Commonly used amine and aminosilane structures

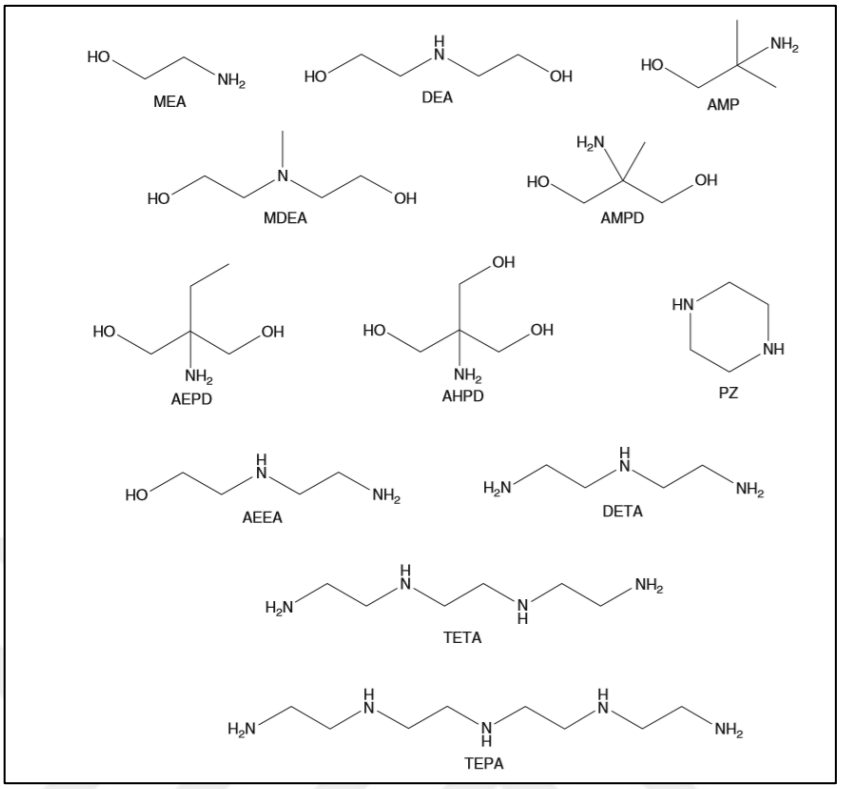

Figure 2.6. Commonly used amine structures(continued)

2.2.3. CO_2 Adsorption over Amine-Functionalized Mesoporous Silica

As mentioned above, amine modified mesoporous silica has attracted great deal of attention in the field of CO_2 capture. Xu et al. were the first to show that branched Polyethyleneimine(PEI)-impregnated mesoporous silica captured higher amounts of CO_2 than bare supports [40]. While 0.2 mmol/g sorbent of CO2 could be adsorbed over the bare support, this value increased up to 3.02 mmol/g when 75 wt. percent PEI was used under pure CO_2 gas stream at 75^oC. Maximum adsorption capacity was obtained as 4.88mmol/g for 50 wt. percent PEI, while only half of these amounts could be captured with pure PEI [3].

Following the pioneering work of Xu et al. extensive amount of research has been conducted over various amine-modified mesoporous silica focusing mainly on the determination of the effects of structural parameters (like pore size, silica type, and etc.), adsorption conditions

(like temperature, pressure, relative humidity), and preparation methods (impregnation, grafting and co-condensation) on the adsorption performance of the developed sorbents.

The sorption capacity of mesoporous silica has been reported to be dependent on the surface amine density as well as the pore size. Wang et al. demonstrated that the pore size of the mesoporous silica had a dramatic effect on the CO_2 capture performance of silica-amine sorbents. Structures with 7.6 nm mesopores showed better CO_2 capture performance than those with 5.6 nm mesopores. Zelenak et al. observed similar findings in their study investigating CO_2 capture over three different molecular sieves. In addition to these, they also reported that higher surface density of amines achieved much higher CO2 adsorption capacities. In the study of Harlick et al., it was observed that pore-expanded MCM-41 with larger pore diameters succeeded in much higher CO2 uptakes compared to that of the conventional MCM-41 with smaller pore diameters. To generalize, capacity of the molecular sieves with larger pores and higher surface amine densities was greater, while the type of the mesoporous silica had no impact on the capacity [4,36,41]. Due to the existence of complicated interactions between many factors, generalizing the findings regarding the impact of amine structural characteristics on the amount of adsorption capacity is quite difficult [42,43].

The effect of temperature, pressure, and relative humidity on the CO_2 adsorption capacity have also been investigated frequently with the purpose of developing high-performance adsorbents operating under flue gas conditions. According to Yildiz et al., the adsorption capacity enhanced smoothly with increasing CO_2 partial pressure, with an optimal range of 0.8 to 1.0 bar [30,43,44]. Sanz et al., on the other hand, reported that the higher the amine density on the support surface, the less effective the pressure on the adsorption capacity. As for the temperature, it was discovered that the CO_2 capture decreased as the temperature increased in agreement with the exothermic nature of adsorption but there were also studies claiming a rise in the adsorption capacity of adsorbents with temperature up to 80°C. Those adsorbents involved high-molecular-weight amine structures like tetraethylenepentamine (TEPA) [45,46]. The effect of humidity on the adsorption performance was also not clear. Although there were studies reporting an increase in the capacity with the introduction of moisture, there were also findings supporting that humidity did not influence the CO_2 uptake [5,41,47].

Preparation techniques have been shown to be quite effective on the adsorption capacity as well. There are three ways to prepare these adsorbents as impregnation, grafting and co-condensation. Due to the low number of amines on the surface and the silica wall, the preparation method with the lowest carbon dioxide adsorption performance is co-condensation. In the grafting method, the amount of loaded amine depends only on the number of surface OH groups, the -OH density on the surface limiting the CO2 adsorption capacity. On the other hand, in the impregnation method, the amount of amine loaded is directly related to the amount of amine used in modification process and the pore volume of the mesoporous silica. Impregnated samples possess significant diffusion issues in case of high-molecular-weight amines and low thermal stability for low-molecular-weight amines [43,46,48].

Although most of the previous studies have concentrated on the determination of the effect of various parameters on adsorption performance, it is equally crucial to figure out how CO_2 capture takes place over amine-functionalized mesoporous silica for the development of highly effective adsorbents.

2.3. CARBON DIOXIDE CAPTURE MECHANISM

2.3.1. Absorption Mechanisms

Interaction of CO_2 with the aqueous amine solutions is an acid-base reaction and has been the subject of a number of experimental and theoretical investigations [49-51]. These studies reported that CO_2 is captured in the form of ammonium carbamates through the well-accepted zwitterion mechanism for primary amines and secondary ones. Reported mechanism shows that, firstly, the lone pair on the nitrogen atom attacks carbon dioxide, forming the zwitterionic intermediate in Equation (2.1) and then this step is followed by the protonation of the zwitterion by another amine molecule giving rise to the formation of an ammonium-carbamate ion pair in Equation (2.2) [49,52,53].

$$R_1NH_2 + CO_2 \leftrightarrow R_1NH_2^+COO^- \quad (2.1)$$

$$R_1NH_2^+COO^- + R_2 \leftrightarrow R_1NHCOO^- + R_2H^+ \quad (2.2)$$

If the amine group is tertiary or sterically-hindered, CO_2 absorption is achieved through the base-catalyzed hydration mechanism of Equation (2.3) in the form of bicarbonates as long as the base functionality is of appropriate strength and can be accessed by the H_2O molecules [51,54].

$$RNH_2 + CO_2 + H_2O \leftrightarrow HCO_3^- + RNH_3^+ \quad (2.3)$$

As it can be deduced from the reaction stoichiometry of the two mechanisms, carbamate formation requires two amine molecules whereas only one amine molecule is sufficient for the formation of bicarbonate. Although tertiary or sterically hindered amines seem to be advantageous in terms of adsorption capacities (due to the reaction stoichiometry), their use is restricted due to their slow kinetics of absorption.

2.3.2. Adsorption Mechanisms

Early studies performed over CO2 adsorption over amine-functionalized solid sorbents assumed that reaction mechanism of CO_2 adsorption was the same as that of absorption in aqueous amine systems so carbamate was the main product under dry conditions while bicarbonate was favored in the presence of moisture. Following spectroscopic results were analyzed accordingly and the findings of those studies were claimed to produce an evidence for the formation of these products.

Leal et al. investigated the CO_2 adsorption over 3-aminopropyl-triethoxysilane (APTMS)-grafted silica gel in the absence and presence of humidity and reported the formation of carbamate species in anhydrous environments and bicarbonate species in case of humid conditions based on the Fourier Transform Infrared Spectroscopy (FTIR) bands identified respectively at 1411 cm-1 and 1385 cm-1. The peak observed at 1596 cm-1 was attributed to the formation of the NH_3^+ species [55].

Chang et al. investigated the adsorption of CO_2 over APTMS modified SBA-15 by using two different gas streams, namely He/H_2O and $CO_2/He/H_2O$. Although no noticeable changes were monitored in the IR spectra under He/H_2O flow, new peaks that were attributed to the formation of bidentate bicarbonate (1634cm^{-1}), bidentate carbonate (1390 cm^{-1} & 1575 cm^{-1}), monodentate bicarbonate (1432 cm^{-1} & 1493 cm^{-1}), monodentate carbonate (1337

cm^{-1}), and carbamic acid (1595 cm^{-1}, 1440 cm^{-1}, and 1330 cm^{-1}) were reported under CO_2 flow. Carbamic acid was proposed to be a precursor for the formation of R-NH_3^+ [56].

Khatri et al., in their study performed over [N-(2-aminoethyl)-3-aminopropyl]trimethoxysilane (AEAPS)-modified SBA-15 under moist He/CO_2/Ar stream, reported the formation of bidentate bicarbonate, bidentate carbonate, and monodentate bicarbonate based on their identification of IR bands found at 1628 cm^{-1}, 1541 cm^{-1}, and 1422 cm^{-1}, respectively. Following this, they carried out another investigation over APTMS SBA-15 involving D_2O and based on the shifts observed in the IR peaks, it was stated that H_2O had a crucial effect on the adsorption mechanism [57,58]. Contrary to these findings, Zhang et al. and Hiyoshi et al. argued that the adsorption mechanism of CO_2 adsorption over [N-(3-trimethoxysilyl)propyl]ethylenediamine (AEAPS)-SBA-15 was unaffected by humidity [5,47].

Although infrared spectroscopy is a frequently applied method in the identification of CO_2 adsorption products and intermediates, IR findings are indeed very open to discussion due to short band overlaps and low densities. The structures specified as bicarbonates and carbonates in the former studies, for example, have later been assigned for different carbamate forms. Wang et al., in their study performed over PEI-functionalized mesoporous silica, claimed that the product identified at 1410 cm^{-1} in anhydrous environment was in fact an alkylammonium carbamate with the assumption that bicarbonate and carbonate formations are not allowed in the absence of moisture. The bands found at 1650 cm^{-1}, 1520 cm^{-1}, 1410 cm^{-1} and 1320cm^{-1} were attributed to the N-H deformations found in RNH_3^+ and the C=O stretch as well as the NCOO skeletal vibration found in alkylammonium carbamate. As a result, alkylammonium carbamate species was proposed to be the main CO_2 adsorption product over PEI-modified mesoporous silica under dry conditions [59].

Bacsik et al., on the other hand, reported the formation of ammonium carbamate, surface-bound carbamate and carbamic acid involved in hydrogen bonding over 3-aminopropyl-methyldiethoxysilane (APMDES) and (3-aminopropyl) triethoxysilane(APTMS) functionalized silica under CO_2 flow in the absence of H_2O [60]. Both ammonium carbamate and carbamic acid species were easily desorbed under vacuum conditions, while carbamates attached to the surface were found to be quite stable. Similarly, Danon et al. mentioned the presence of alkyl ammonium carbamates and surface-bound carbamate products in their study carried out over APTMS-grafted SBA-15 under dry conditions. When benzylamine

spacer was used to form isolated amine groups and the mechanism between a single amine and CO_2 was investigated, it was observed that only surface-bound carbamates were formed. Accordingly, it has been proposed that these surface-bound carbamates were formed as a result of the interaction of intermediate carbamic acid structures with surface OH groups. When these OH groups were not available, no CO_2 adsorption could be observed underlining the significant role of the surface OH groups in CO_2 capture [61]. The FTIR spectra over SBA-15 modified with acrylonitrile-modified tetraethylenepentamine (TN) was studied by Zhang et al. and the bands observed at 1411cm^{-1} and 1313cm^{-1} were assigned to the NCOO bending of zwitterion observed in the generally accepted zwitterion mechanism for CO_2 capture [62].

Nuclear magnetic resonance(NMR) spectroscopy has also been a frequently-used method in experimental research due to the disagreements noticed in IR findings. The first study working with solid state NMR to examine the species formed during CO_2 adsorption was published by Pinto et al in 2011 by using APTMS-grafted PCH (porous clay heterostructures). The single peak identified at 125 ppm was attributed to the physically-adsorbed CO_2 whereas the peaks observed at 160 ppm and 164 ppm were considered as carbamic acid and carbamate species, respectively; resulting from the interaction of CO_2 with surface amines [63]. Moore et al. investigated the adsorption mechanism of CO_2 over a hyperbranched aminopolymer (HAS) that involved primary, secondary and tertiary amine groups. Both of these materials are known to adsorb CO_2 at a temperature range of ambient to 120°C. Due to the presence of different amine functionalities, carbamic acid (160ppm), carbamate (164ppm) and bicarbonate (163ppm) formations were reported to be observed during adsorption[64]. Mafra et al. investigated CO_2 capture over APTMS (primary amine), MAPS(secondary amine), ([3-(diethylamino)propyl]trimethoxysilane (DMAPS (tertiary amine)), and N-[3-(trimethoxysilyl)propyl]ethylenediamine (AEAPS (diamine))-functionalized SBA-15 by using solid state NMR and DFT modelling. An additional peak identified at 153 ppm only in extremely dry environments was attributed to the presence of an isolated carbamic acid structure and this was supported by DFT calculations as well. The resonance at 160 ppm was also associated to a carbamic acid but different from the previous structure, this was involved in two or more hydrogen bonds. The resonance at 164 ppm was assigned to an alkyl ammonium carbamate structure as before. However, DFT simulations demonstrated that the propylammonium carbamate ion pair was energetically unfavorable

[65]. Similarly, Foo et al. studied CO_2 adsorption over APTMS, MAPS, and DMAPS-functionalized SBA-15 and reported the presence of NMR peaks identified at 164.6 ppm (ammonium carbamate) and 160.8 ppm (carbamic acid) in case of APTMS and MAPS. APTMS-carbamic acid involved hydrogen bonds between the surface silanols and OH group of carbamic acid, while there were two MAPS-carbamic acid structures, the first one being hydrogen bonded to a neighboring amine and the second one being hydrogen bonded to the neighboring carbamic acid. For DMAPS, only bicarbonate formation was observed. Bicarbonate formation could not be observed for APTMS and MAPS.

Aziz et al. argued that the amount of ammonium carbamate formation decreased significantly when a certain distance between amine groups is exceeded in case of APTMS-modified mesoporous silica particles [66]. Cendak et al. conducted a similar study examining the effect of amine-amine distance on the adsorption mechanism using APTMS-SBA-15. Three different models namely with high amine loading**,** low amine loading**,** and very low amine loading (isolated amines) were investigated; the surface amine density for each model being 2.8mmol/g, 0.9mmol/g and 0.5mmol/g, respectively. Solid state NMR results showed three resonances at 154 ppm,160 ppm and 164 ppm which were named as A, B, and C, respectively. Species A was dominant in case of the low and very low density samples and was proposed to be an isolated carbamic acid structure that was interacting with surface silanols in conjunction with the Density Functional Theory(DFT) calculations [67].

Cho et al. reported that the surface silanols affected the stabilization of carbamate ions on APTMS functionalized mesoporous silica systems. In this work three different thermodynamically feasible mechanisms were reported, namely intermolecular mechanism, surface mechanism and water assisted intermolecular mechanism. It has been shown that hydrogens of surface silanol groups are actively involved in proton transfer during the surface mechanism. For the intermolecular mechanism, surface silanols played no role in the carbamic acid formation, there was a simultaneous H transfer from the CO2-adsorbed amine to the neighboring one and from this neighboring amine to the CO2 molecule. In the presence of H2O, on the other hand, proton transfer can originate from H_2O. The fact that the required activation energy is lower in the surface mechanism indicates that CO2 is captured through this pathway under dry conditions [68].

Very recently, Topçubaşı investigated the CO_2 adsorption mechanism over APTMS (primary)-functionalized mesoporous silica by using DFT. Five different reaction

mechanisms, direct carbamate, direct carbamic acid, carbamate to carbamic acid, carbamic acid to another carbamic acid and isolated carbamic acid formation mechanisms were identified for 5_5 APTMS. Among them, the pathway involving the formation of carbamic acid through carbamate and carbamic acid from an another carbamic acid are found to be thermodynamically feasible. In the other three infeasible routes, hydrogen bonding did not occur with the surface silanols but in some cases with the neighboring amine, however these interactions were not sufficient for the stabilization of the final product. For 5_4_5 APTMS which has a higher number of the surface silanol groups and lower amine density, six different mechanisms were found according to the reaction pathway studies. The zwitterion structure was observed in all reaction mechanisms found. This is because of the complex hydrogen bonding networks formed by the increased surface silanol groups. The carbamate to carbamic acid formation through the zwitterion (ZCBA) mechanism whose end product was a carbamic acid has been found as the most energetically feasible pathway. The end product contained hydrogen bonding interactions with both the surface and the adjacent amine. Surface-mediated mechanisms were also reported where surface -OH groups played a direct role in the reaction pathway as reported previously by Cho et al. [68,69].

2.4. MOLECULAR MODELLING

Molecular modeling is a method of calculating energies of molecular structures in order to determine motions or positions of 3-D structures using classical and quantum physics, being still the only method that can identify the nature of chemicals at the molecular scale. Molecular modeling is used to support experimental results in areas such as catalysis, materials science, and drug design.

Molecular modeling methods may be classified in two main groups regarding the type of physics involved. Molecular mechanics uses Newton mechanics to model a particular system with the potential energy of the system being calculated as a function of the nuclear coordinates using the force fields. Molecular dynamics, on the other hand, deals with the time-dependent physical movements of atoms and molecules by solving Newton’s equations of motion. These methods can be used for even very large systems without requiring high computational cost and can still provide useful information about equilibrium geometries and conformations while they are insufficient in handling chemical reactions.

Quantum mechanical calculations, on the opposite, are based on the solution of the Schrödinger's equation and provide information about the electron distributions within a chemical structure. Because quantum chemical calculations are more detailed and more precise, huge computational investments are required for the calculation of large systems and the complexity of the method makes calculations quite time-consuming compared to molecular mechanics [70,71].

A quantum-mechanical system's wave function is defined by the Schrödinger equation (Equation 2.4), which is a linear partial differential equation. Since the exact solution is only for the hydrogen atom, only approximate results can be obtained in multiple systems. For multiple systems, Schrödinger equation can be expressed as follows;

$$\hat{H}_{\psi}=E_{\psi} \tag{2.4}$$

Where $\hat{H}_{\psi}$ represents the Hamiltonian operator, E represents the electronic energy and ψ represents wave functions. Hamiltonian operator includes five different parameters (Equation 2.5) that stands for the kinetic energies of the electron and the nuclei, attraction of electrons by nuclei and also interelectronic/internuclear repulsions.

$$\hat{H}_{\psi}=-\frac{1}{2}\sum_{i}^{electrons}\nabla_{i}^{2}-\frac{1}{2}\sum_{A}^{nuclei}\frac{1}{M_{A}}\nabla_{A}^{2}-\sum_{i}^{electrons}\sum_{A}^{nuclei}\frac{Z_{A}}{r_{i,A}}+\sum_{i<j}^{electrons}\sum\frac{1}{r_{ij}}+\sum_{A<B}^{nuclei}\sum\frac{Z_{A}Z_{B}}{R_{AB}} \tag{2.5}$$

With the Born-Oppenheimer approximation, the kinetic energy of the nucleus is negligible and nuclear positions can be excluded from being considered as variables that cancels the second term of the Hamiltonian operator. The equation becomes more simplified by using an additional Hartree-Fox approximation that claims that each electron's motion can be described by a single particle orbital which does not depend on the other electrons and in this way the Hamiltonian is simplified to Equation (2.6).

$$\hat{H}_{\psi}=-\frac{1}{2}\sum_{i}^{electrons}\nabla_{i}^{2}-\sum_{i}^{electrons}\sum_{A}^{nuclei}\frac{Z_{A}}{r_{i,A}}+\sum_{i<j}^{electrons}\sum\frac{1}{r_{ij}} \tag{2.6}$$

This results in a set of coupled differential equations for each electron and the Linear Combination of Atomic orbitals approach which is a quantum superposition of atomic orbitals and a method for defining molecular orbitals in quantum chemistry converts the differential equations to an easy-to-solve algebraic equations [72].

2.4.1. Density Functional Theory Method

DFT is a calculation type of electronic structures which is based on the fact that ground state wave function is a unique functional of the charge density. Accordingly, it uses functionals of electron density instead of dealing with many-body wavefunction. The total electronic energy may be written as the sum of several terms:

$$E = E_T + E_V + E_j + E_{XC} \tag{2.7}$$

where E_T is the total kinetic energy of the electrons, E_V is the total potential energy due to Coulomb attraction of electrons to the nuclear centers, E_j is the total potential energy due to Coulomb repulsion between electron pairs, E_{XC} is the total exchange and correlation energy that accounts for all the remaining electron-electron interactions [72]. All the terms except for the kinetic energy are dependent on the electron density (n(r)) which can be expressed as:

$$n(r) = 2 \sum_{i=1}^{\text{orbitals}} (|\psi_i(r)|)^2 \tag{2.8}$$

where ψ_i are the Kohn-Sham orbitals. Calculation of the ground state energy is achieved through the solution of Kohn-Sham equations which are obtained through the determination of the unknown coefficients of the orbitals that would minimize the total electronic energy.

Among the terms involved in the total electronic energy, the exact form of the exchange and correlation energy is unknown so an approximation is needed. These approximations can be grouped in three, namely local density approximation(LDA), generalized gradient approximation (GGA) and exact Hartree-Exchange [72].

The local density approximation (LDA) treats the local density as a homogeneous electron gas and assumes that density fluctuations are gradual. Because the LDA approximates the real density's energy by the energy of a local constant density, it fails in circumstances where the density fluctuates rapidly, such as in molecules. This can be improved by taking the gradient of the electron density into account which is known as the Generalized Gradient Approximation (GGA). The Hartree–Fock model, on the other hand, implies that the exact

N-body wave function of the system can be roughly estimated by a single Slater determinant [73].

2.4.2. Basis Sets

The linearly combined functions that are used to model the molecular orbitals of molecules is called the basis set. Basis set can be composed of atomic orbitals for quantum chemistry; plane waves for solid state and real-space calculations. There are three types of atomic orbitals that can be used: Gaussian orbitals, Slater orbitals, and numerical atomic orbitals. In the linear combination of atomic orbitals molecular orbital method, Slater-type orbitals (STOs) are functions that are employed as atomic orbitals [72,74]

Since calculations with hydrogen functions were not efficient, Slater atomic orbitals, briefly STOs, were used. Since STO-3G includes the atoms that make up the molecule and only spherical functions, the STO-3G basis set was insufficient to identify non-spherical molecules and their electron distributions [72]. While molecular bonds are considered, valence electrons are represented by more than one basis function since usually valance electrons take part in bonding. Since the valence orbitals are divided into two (or more) fundamental functions, such fundamental sets are called "split valence" basis sets.

The Gaussian basis set is denoted by the abbreviation N-MPG* where N represents the number of Gaussian primitives used for each inner shell orbitals, M represents the number of primitives that make up the large zeta function for the inner valence region, and P represents the number of primitives that make up the small zeta function for the outer valence region [72].

For the most accurate modeling of orbitals, the largest basis set should be used. Since using the largest basis set will cause both time and computational cost in calculations, optimization should be made in terms of time and computational cost.

3. COMPUTATIONAL WORK

3.1. COMPUTATIONAL MODELS

Two different molecular structures of trimethoxy[3-(methylamino)propyl]silane (MAPS)-modified mesoporous silica with different amine densities were used in this study, as previous studies proved that surface amine density as well as the surface silanol density were quite deterministic on the CO_2 adsorption capacities and mechanisms [65,75-77].

MCM-41 is one of the most frequently investigated mesoporous silica structure for CO_2 capture, the pore walls of which are made of amorphous silica. Due to the huge size of the MCM-41 structure, it was impossible to model the whole system and two different SiO2 clusters (denoted as 5_5 and 5_4_5) varying in size were chosen to represent the mesoporous silica. The smaller cluster (Figure 3.1) involved eight SiO2 groups in total in the form of two connected five-membered rings while the other one (Figure 3.2) was built of two connected five-membered and one four-membered rings with 10 SiO_2 groups in total. The terminal oxygen atoms were saturated with hydrogens.

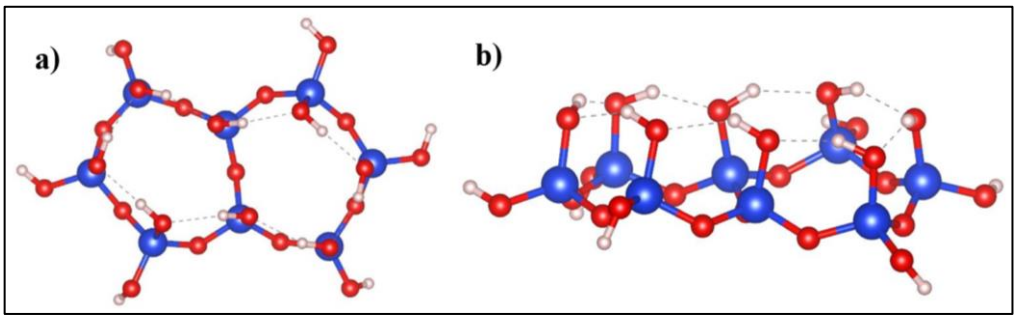

Figure 3.1. a) top view of small 5_5 model, b)side view of small 5_5 model

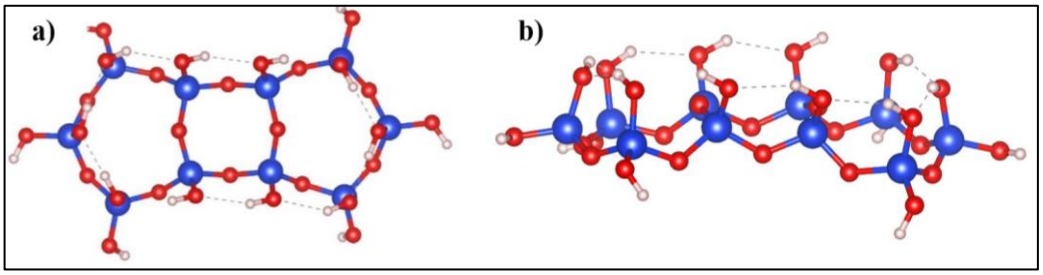

Figure 3.2. a) top view of 5_4_5 model, b)side view of 5_4_5 model

MAPS is among the most-widely investigated amines for CO_2 adsorption that involves a secondary amine group. MAPS-MCM41 models were created through the attachment of two MAPS molecules onto the surface of SiO_2 clusters through a condensation reaction taking place between the $–OCH_3$ groups of each MAPS molecule and the surface silanols giving three CH3-OH molecules off. Molecular structures of 5_5-MAPS-MCM41 and 5_4_5-MAPS-MCM41 models are given in Figure 3.3 and Figure 3.4, respectively. The surface amine densities of the two models were calculated as 4.52 and 3.40 molecules/nm2 for 5_5 and 5_4_5 models, respectively and found by dividing the number of amine groups involved in the structure by the surface area of the mesoporous silica. The surface area of the mesoporous silica was obtained by multiplying the maximum Si-Si distances in the x and y directions.

Next, conformational analysis of both models were performed by using Molecular Mechanics and of the 6561 conformers obtained for each model, various structures that could lead to different CO_2 adsorption pathways were selected for further consideration in reaction pathway analysis.

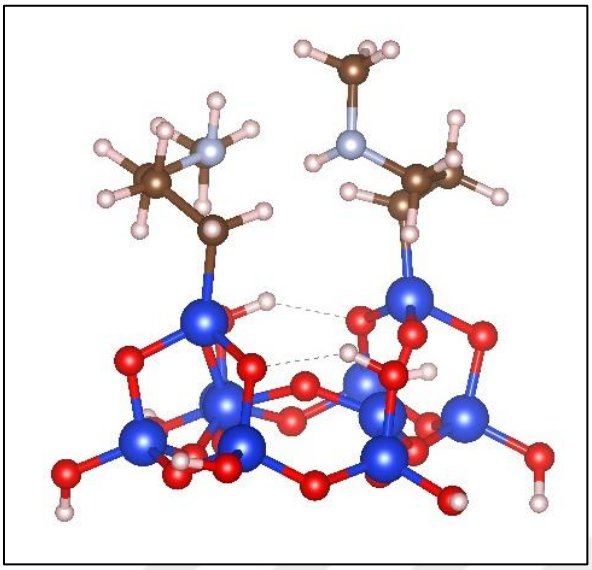

Figure 3.3. Conformer 4013 MAPS-MCM41 for 5_5 model

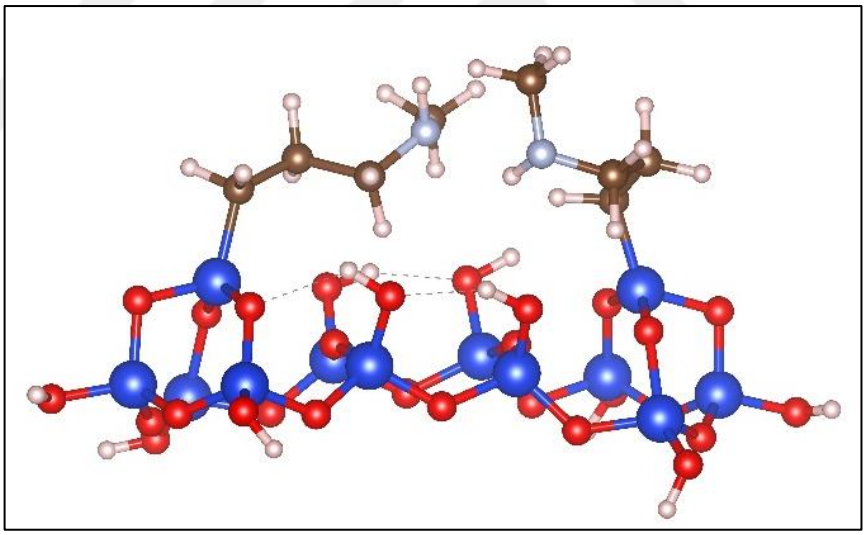

Figure 3.4. Conformer 3527 MAPS-MCM41 for 5_4_5 model

3.2. COMPUTATIONAL PARAMETERS

Conformational analysis was executed using Molecular Mechanics of Avogadro 1.2.0 software [78] with the MMFF94 force field, whereas the reaction pathway analysis was performed through the DFT of Gaussian 16 [79]. Becke's three parameter hybrid functional (B3LYP) [80] was the exchange correlation functional and the basis set was 6-31G(d) [81].

Dispersive interactions were taken into account by using Grimme's D3 dispersion correction scheme [82].

3.3. COMPUTATIONAL METHODOLOGY

To examine the reaction mechanism of CO_2 using MAPS-functionalized mesoporous silica, the creation and selection of the amine modified silica clusters were achieved first. Following this, reaction pathway analysis was performed using three main types of calculations, i.e. transition state searches, geometry optimizations, and intrinsic reaction coordinate (IRC) calculations.

Lowest-energy structures of all the identified structures (i.e. reactants, products and intermediates) together with their energies were obtained through geometry optimizations whereas the transition state geometries were attained using the QST2 method of the Synchronous Transit-Guided Quasi-Newton (STQN) algorithm of Gaussian 16. Frequency calculations were always executed after each optimization and QST2 run, in order to confirm that the obtained structure was either a global minimum or a transition state. Subsequent to the identification of transition states, IRC calculations were run for the confirmation of the obtained geometries. All the energies are given in terms of free energies, being calculated with the thermochemical data provided by the Gaussian calculations.

Eventually, to simulate the mechanical fixing supplied by the vast number of SiO_2 units involved in a real MCM41 molecule, the two MAPS molecules included in the molecular models together with the six Si-O-Si bonds and the free standing surface silanol groups and CO_2 (if present) were fully relaxed during the calculations while all the remaining atoms were fixed.

4. RESULTS AND DISCUSSION

As it was discussed in the previous section, two different mesoporous silica models (5_5 and 5_4_5) were used for the generation of MAPS-functionalized adsorbents resulting in two different surface amine (4.52 molecules/nm^2 and 3.40 molecules/nm^2, respectively) and surface silanol densities. Accordingly, the findings regarding the CO_2 adsorption mechanism over MAPS-MCM-41 will be discussed in two main sections, namely 5_5-MAPS and 5_4_5-MAPS.

4.1. REACTION PATHWAY ANALYSIS OVER 5_5-MAPS

When two MAPS molecules were grafted onto the surface of 5_5 mesoporous silica model, there were 2 free surface silanols remaining at the surface. Due to the small number of silanols and the sterically-hindered nature of the MAPS molecule, the interaction of the amine molecules with the surface was found to be quite restricted when compared to the case of APTMS that was previously reported by Topcubasi [69].

Several different conformers were taken into consideration for the examination of CO_2 adsorption and three distinct pathways which are direct carbamate formation (DCB), direct carbamic acid formation (DCA), and isolated carbamic acid formation (ICA) were determined over the structures considered. Reaction energy diagrams of the 3 paths are summarized in Figure 4.1; reference state (REF) in the energy diagrams being the sum of the free energies of gaseous CO_2 and the corresponding 5_5-MAPS conformer.

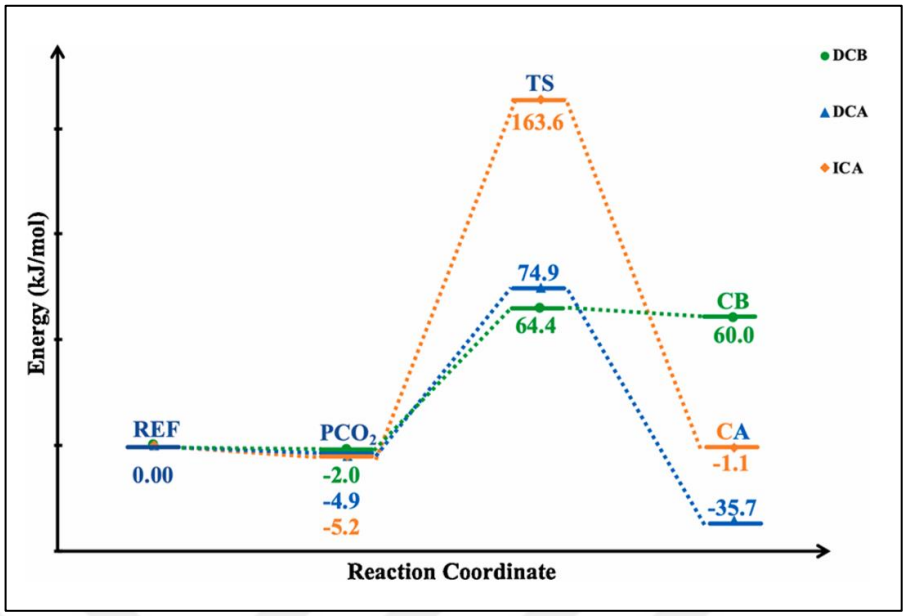

Figure 4.1. Reaction energy diagrams of CO_2 adsorption over 5_5-MAPS. REF: Reference state, PCO_2: Physisorption state, TS: Transition state, CA: Carbamic acid, and CB: Carbamate [83]

4.1.1. Direct Carbamate Formation Route (DCB)

According to the DCB mechanism (Figure 4.2), physically adsorbed CO_2 was transformed directly into an ammonium carbamate ion pair by the deprotonation of the CO_2-adsorbed amine by the neighboring amine molecule. Estimated activation barrier for this step was 66.4 kJ/mol while the physisorption energy of CO_2 was 2.0 kJ/mol. The ion pair that was formed (Figure 4.3) had no interactions with the silanols on the surface but the two amine molecules were involved in hydrogen bonding through the transferred proton. Due to the limited hydrogen bonding interactions, the resulting ammonium carbamate pair was calculated to be 60.0 kJ/mol less stable compared to the reference point (MAPS-MCM-41 + CO_2) indicating that the identified pathway was thermodynamically infeasible. Molecular structures of the CO_2 adsorption species of the DCB mechanism are given in 4.3.

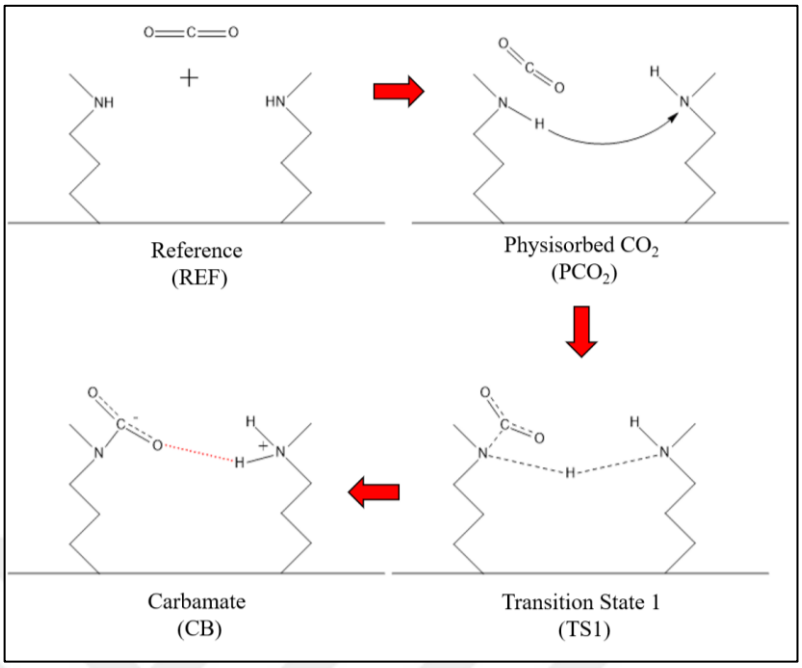

Figure 4.2 Schematic drawing of the 5_5 MAPS DCB mechanism

Topcubasi previously mentioned a similar pathway over 5_5-APTMS (primary amine) [69]. Our findings regarding the reaction energetics of CO_2 adsorption over MAPS-functionalized mesoporous silica were very close to the previously reported values of adsorption energy (-4.9 kJ/mol), activation barrier (68.7 kJ/mol) and relative stability of the product (69.6 kJ/mol) for APTMS [83].

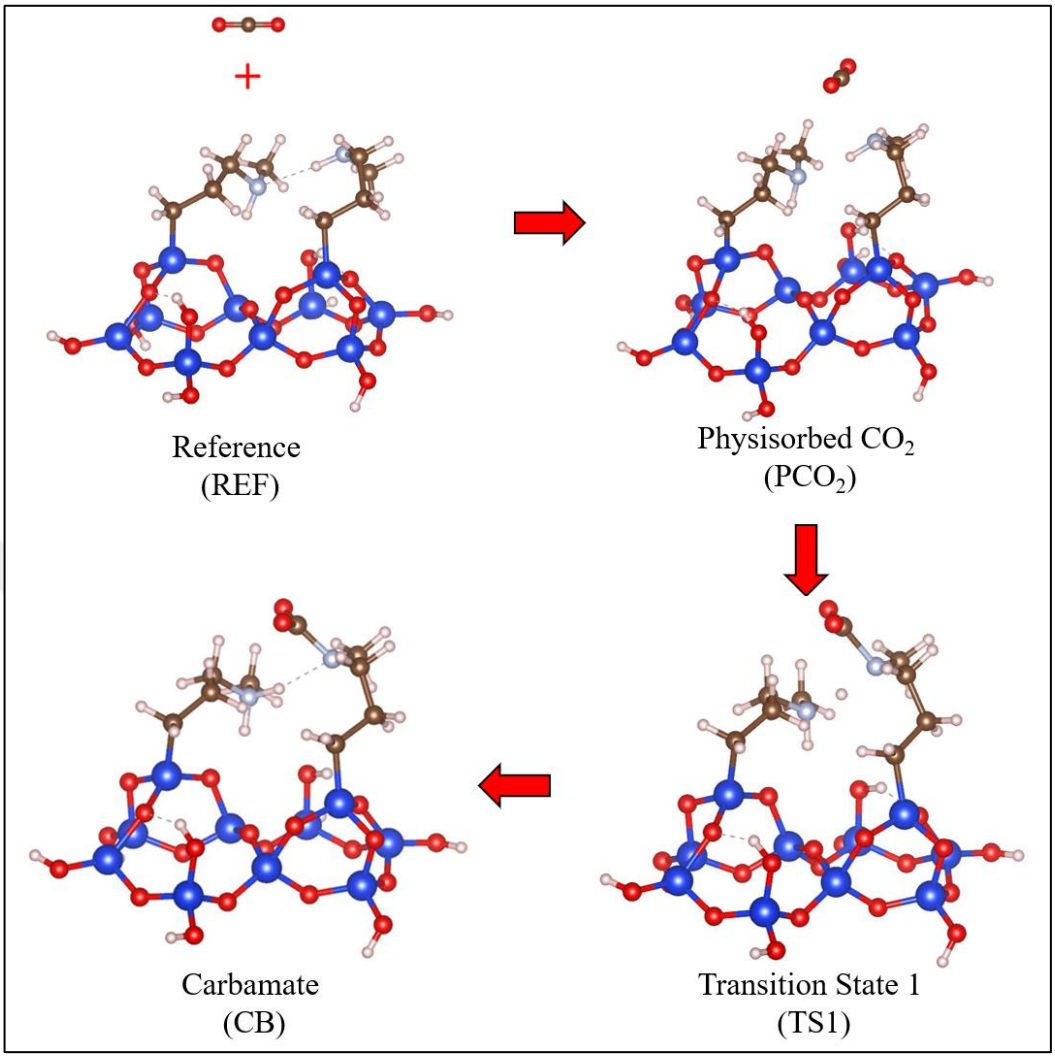

Figure 4.3. Molecular structures of the CO_2 adsorption species of the 5_5 MAPS DCB mechanism

4.1.2. Direct Carbamic Acid Formation Route (DCA)

In the DCA mechanism, CO_2 was physisorbed at the surface with an adsorption energy of 4.9 kJ/mol that was followed by the transformation of this adsorption complex into a carbamic acid with an activation barrier of 79.8 kJ/mol (Figure 4.1). This transformation took place through the simultaneous migration of a proton from the CO_2-adsorbed amine to the neighboring nitrogen atom and another proton from this neighboring amine to the closest oxygen atom of the physically adsorbed CO_2, as can be seen in Figure 4.4. The resulting carbamic acid molecule (Figure 4.5) was hydrogen bonded to the nitrogen of the neighboring

amine structure by its –COH group and was calculated as 35.7 kJ/mol more stable compared to the reference point underlining the thermodynamical feasibility of the reaction mechanism. Previous studies reported the presence of different carbamic acid structures that differed from one another in their stabilities and the hydrogen bonding network in which they are involved [65,69]. Accordingly, the carbamic acid structure observed here was denoted as Type I carbamic acid in order to distinguish it from the other carbamic acid structures that might be discovered in the forthcoming adsorption mechanisms.

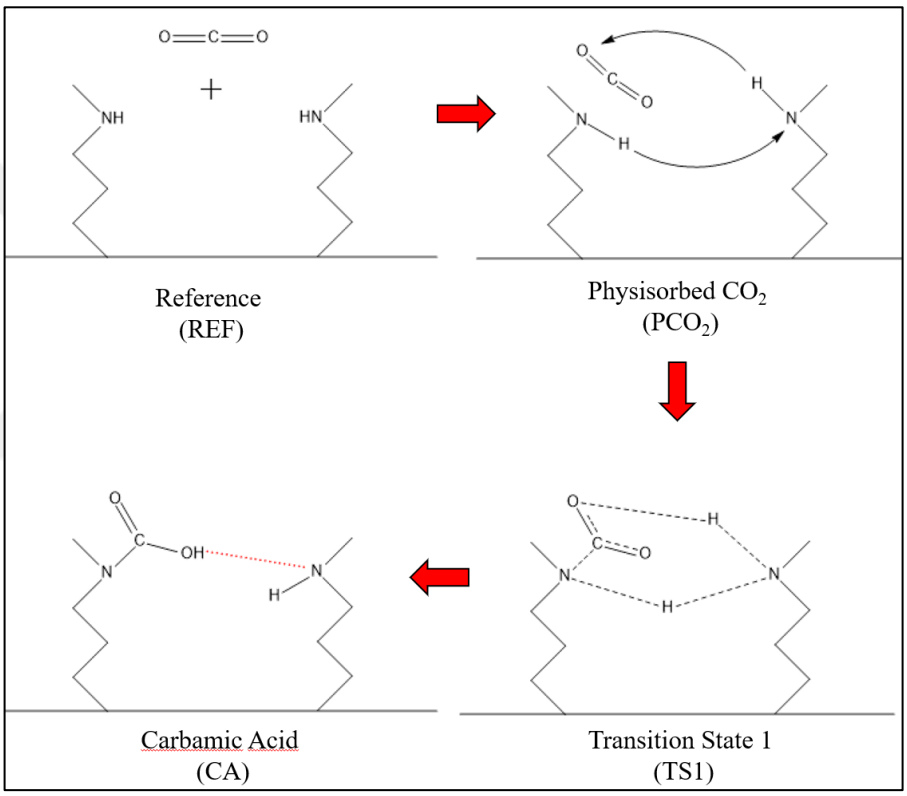

Figure 4.4 Schematic drawing of the 5_5 MAPS DCA mechanism

The physisorption energy and the activation barrier calculated here were close to the values reported for APTMS (3 kJ/mol and 67.3 kJ/mol, respectively) before and both carbamic acid structures were of type I [69]. However, MAPS carbamic acid (-35.7 kJ/mol with respect to the reference point) was found to be more stable than APTMS carbamic acid (5 kJ/mol with respect to the reference point). Although the hydrogen bonding interactions in both structures were limited, = CO group of the MAPS carbamic acid was located close to the surface, near a surface silanol, with an O25-H2-O17 angle of 124.4^{O} and an O25-H2 distance of 2.76 Å

(Figure 4.5). The increased stability of the MAPS carbamic acid might be due to this proximity of the product to the surface or stronger interaction of CO_2 with secondary amines as proposed by previous studies [84].

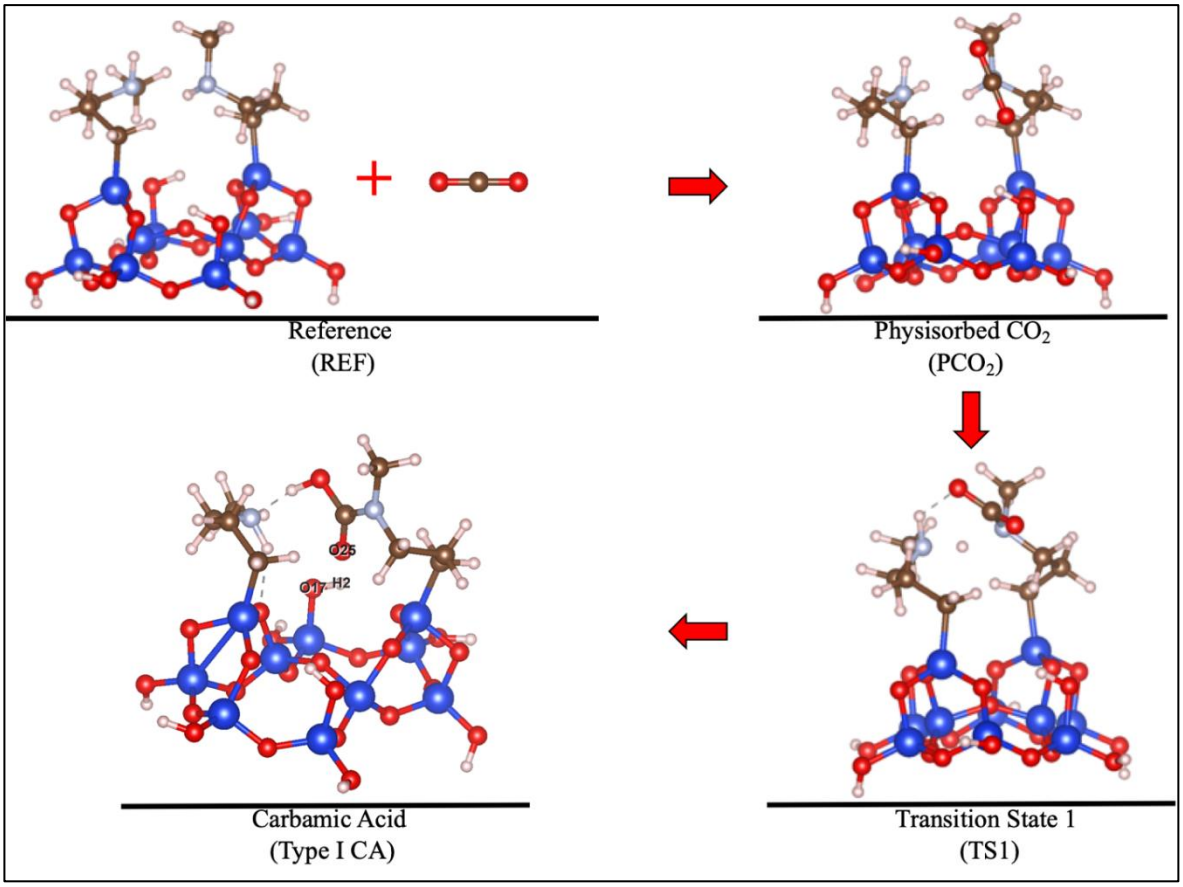

Figure 4.5. Molecular structures of the CO_2 adsorption species of the 5_5 MAPS DCA mechanism

4.1.3. Isolated Carbamic Acid Formation Route (ICA)

Different from the DCA and DCB mechanisms, ICA pathway was found to take place without the requirement of the neighboring amine. Hence, this mechanism was observed over both isolated amine molecules and paired amine molecules without the contribution of the second amine group. According to the reaction energy diagram of the ICA mechanism (Figure 4.1), physisorbed CO_2 (relative energy of -5.2 kJ/mol with respect to the reference) was converted into a carbamic acid molecule through an intramolecular transfer of proton

from the CO_2-adsorbed amine to one of the =CO groups of the CO_2. The required activation energy was calculated as 168.8 kJ/mol, which was significantly higher than the barriers calculated for DCA and DCB pathways; and the final product was 1.1 kJ/mol more stable compared to the reference state. Obtained carbamic acid was of type I. The schematic diagram of the ICA mechanism is given in Figure 4.6.

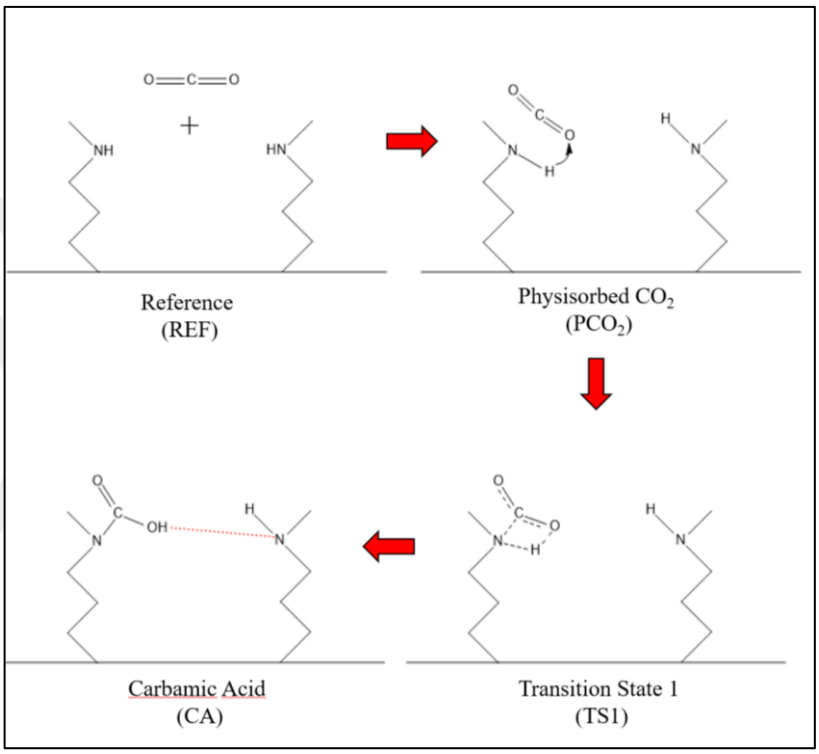

Figure 4.6 Schematic drawing of the 5_5 MAPS ICA mechanism

Both the activation barriers and physisorption energies estimated for 5_5-MAPS were comparable to the values obtained formerly for 5_5-APTMS [69], whereas the carbamic acid observed here was slightly more stable than that of APTMS (relative energy of 12.1 kJ/mol with respect to the reference). This seemed to be originating from the fact that APTMS-carbamic acid had no hydrogen bonding interactions while MAPS-carbamic acid was hydrogen bonded to the neighboring amine through its –COH group. In both cases, activation barriers were extremely high, indicating the slow reaction kinetics of the ICA mechanism. Molecular structures of the CO_2 adsorption species of the ICA mechanism are presented in Figure 4.7.

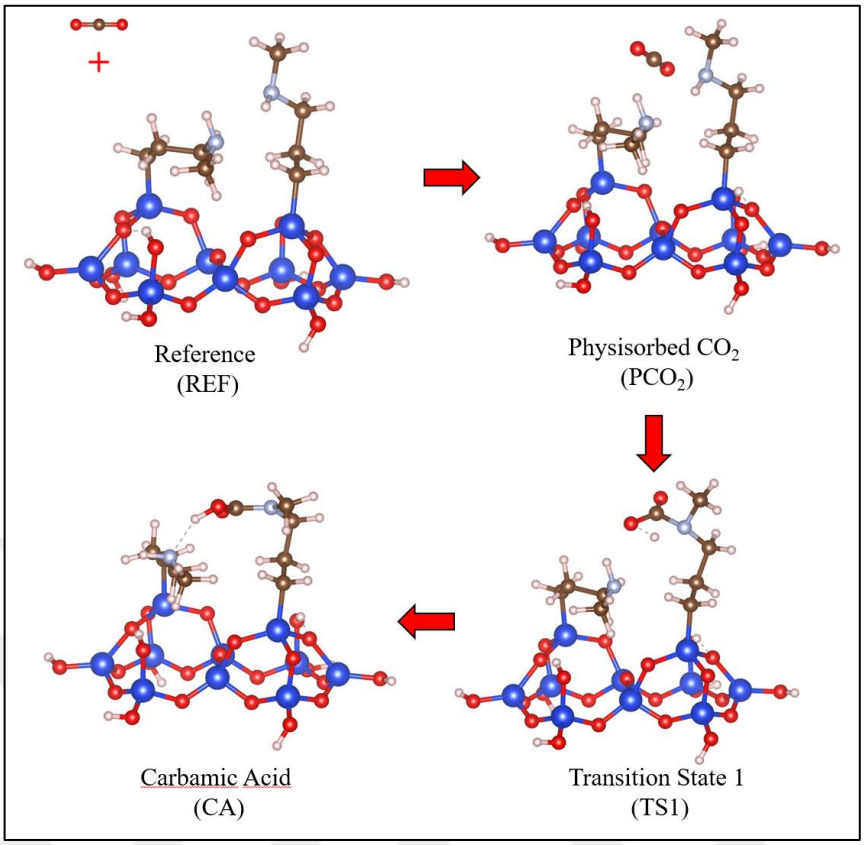

Figure 4.7. Molecular structures of the CO_2 adsorption species of the 5_5 MAPS ICA mechanism

Taking the previous calculations performed over 5_5-APTMS into consideration [69], it may be suggested that the interactions of the adsorption species observed over 5_5-MAPS with the surface were more restricted, probably originating from the increased steric hindrance over the amine due to the -CH3 group bonded to the secondary amine [85]. As a result, only the ICA, DCA, and DCB mechanisms were observed which proceeded without the surface interactions. Despite of the absence of the stabilizing effect of these interactions in case of 5_5-MAPS, the energetics of the identified pathways were similar to that of the same mechanisms observed over 5_5-APTMS.

Among the three CO_2 adsorption pathways identified over 5_5-MAPS, only the DCA mechanism was thermodynamically feasible. The activation barrier calculated for the mechanism was not that low (79.8 kJ/mol) indicating that the main product observed over 5_5-MAPS was carbamic acid of type I but this did not form readily.

4.2. REACTION PATHWAY ANALYSIS OVER MODEL 5_4_5

When two MAPS molecules were grafted onto the surface of the 5_4_5 model, there were four free silanols remaining at the surface. Besides, surface amine density calculated for the 5_4_5-MAPS was less than that of the 5_5 model allowing the MAPS molecules to bend over the mesoporous silica surface more easily. Consequently, the interaction of the amine molecules with the surface was expected to be much more pronounced with respect to the 5_5 models.

Similar to the previous case, several different conformers were examined for the analysis of CO_2 adsorption and nine different routes were found. In addition to the DCA, DCB and ICA mechanisms that were observed in case of 5_5-MAPS too, carbamate to carbamic acid formation (CBA), zwitterion to carbamic acid formation (ZCA), zwitterion to carbamate formation (ZCB), surface-mediated carbamate to carbamic acid formation (SCBA), surface-mediated carbamate to carbamic acid formation through an intermediate (SCBIA), and surface-mediated carbamic acid formation through zwitterion (ZCBSA) mechanisms were identified. Figure 4.8 presents the reaction energy diagrams of the CO_2 adsorption paths over 5_4_5-MAPS but DCB, ZCB and ICA routes, being thermodynamically infeasible, were excluded in the figure to simplify the energy diagram. REF in the energy diagrams denotes the reference state and is made of the sum of the free energies of gaseous CO_2 and the corresponding 5_4_5-MAPS conformer.

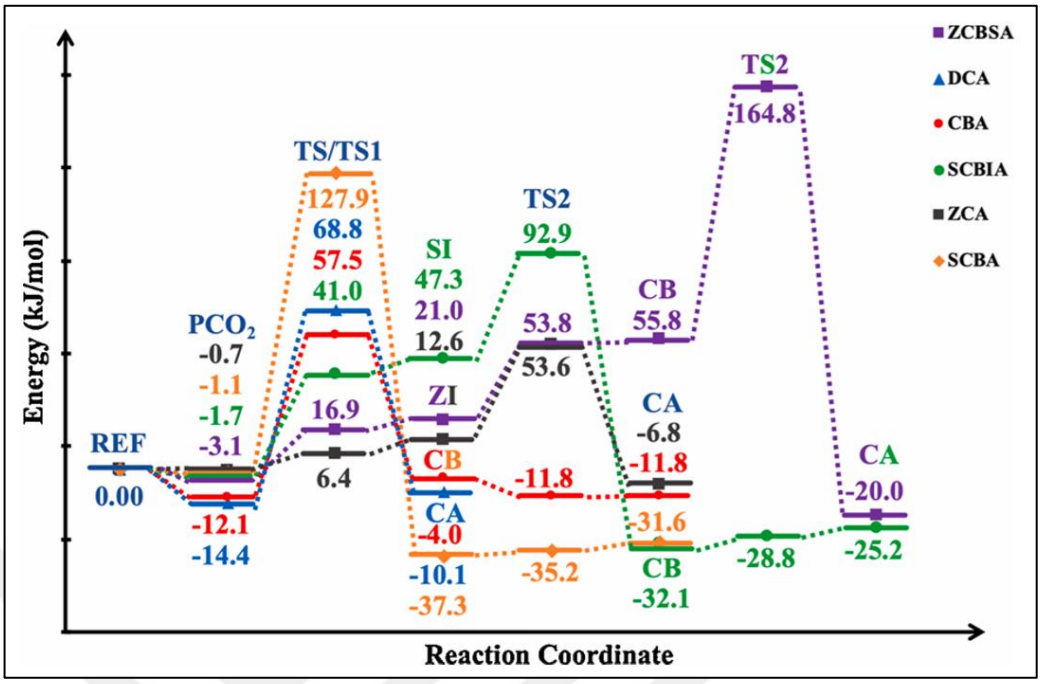

Figure 4.8. Reaction energy diagrams of CO_2 adsorption over 5_4_5-MAPS. REF: Reference state, PCO_2: Physisorption state, TS: Transition state, CA: Carbamic acid, and CB: Carbamate [83]

4.2.1. Direct Carbamate Formation Route (DCB)

DCB mechanism was one of the pathways resulting in a thermodynamically-unfavorable ammonium carbamate end-product. According to the observed mechanism, physically adsorbed CO_2 was transformed into an ammonium carbamate ion pair through the deprotonation of the CO_2-adsorbed amine by the neighboring one (Figure 4.2). This required an activation barrier of 64.7 kJ/mol (Figure 4.8), which was comparable to the value (66.4 kJ/mol) obtained over 5_5-MAPS. Physisorption energy, on the other hand, was calculated as 12. 9 kJ/mol and this was slightly higher than that of the 5_5-MAPS (2 kJ/mol). Although the resulting carbamate structure was hydrogen bonded to one of the free surface silanols through its =CO group and to the neighboring amine through the transferred proton, it was found to be 53.8 kJ/mol more unstable compared to the reference state, similar to the smaller model (calculated relative energy was 60 kJ/mol with respect to the reference). Molecular structures of the reaction species of the DCB mechanism over 5_4_5-MAPS are given in Figure 4.9.

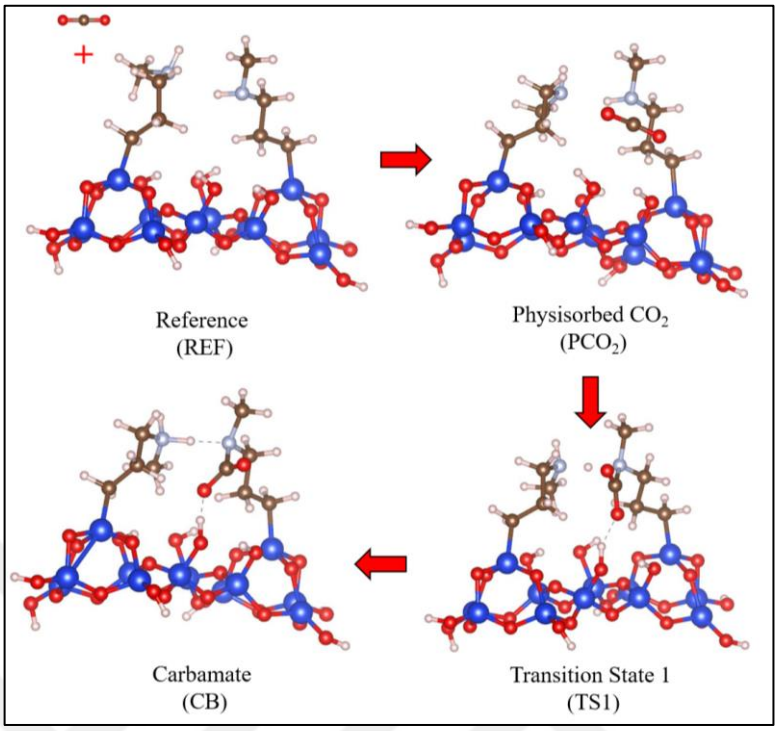

Figure 4.9. Molecular structures of the CO_2 adsorption species of the 5_4_5-MAPS DCB mechanism

4.2.2. Zwitterion to Carbamate Formation Route (ZCB)

Different from the DCB path, in ZCB mechanism (Figure 4.10) carbamate formation proceeds through the creation of the zwitterionic intermediate. According to the identified path, firstly, physisorbed CO_2 was transformed into a zwitterionic intermediate with an activation barrier of 26.3 kJ/mol. This was followed by the deprotonation of this intermediate by the neighboring amine to produce the ammonium carbamate ion pair with a barrier of 19.0 kJ/mol. As it is clear from the calculated activation barriers, formation of the zwitterionic intermediate due to the increased surface interactions caused a significant decline in the required barriers.

Physisorption energy was calculated as 15.0 kJ/mol, which was higher than that of the 5_5-MAPS. Relative energies of the zwitterion and the end-product were, on the other hand, estimated as 13.6 kJ/mol and 34.3 kJ/mol, respectively compared to the reference point representing that both structures were thermodynamically unstable despite of the hydrogen

bonding interactions of both structures with the surface silanol and the neighboring amine. Molecular structures of the reaction species of the ZCB mechanism are given in Figure 4.11.

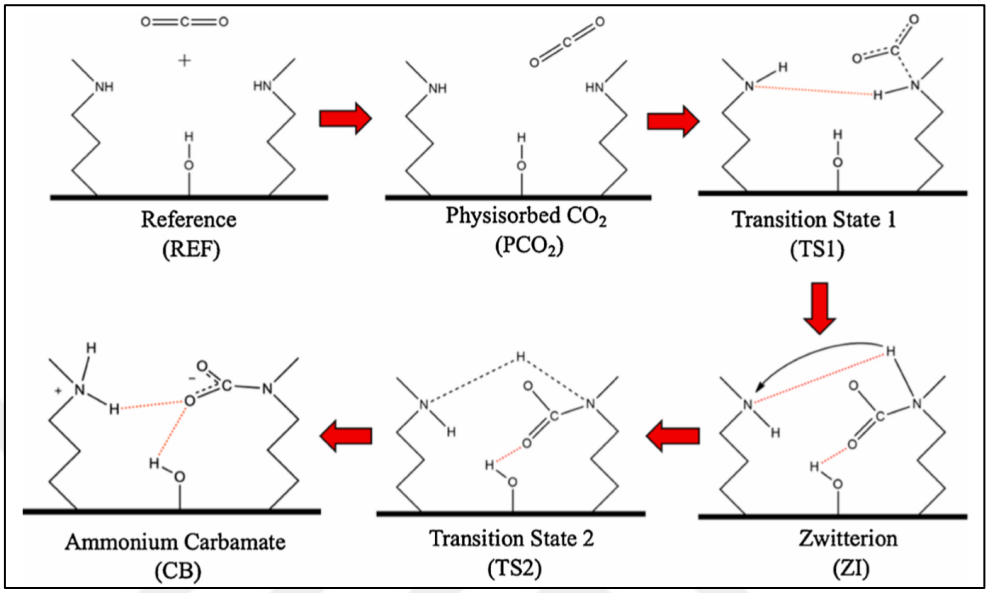

Figure 4.10. Schematic drawing of the 5_4_5-MAPS ZCB mechanism

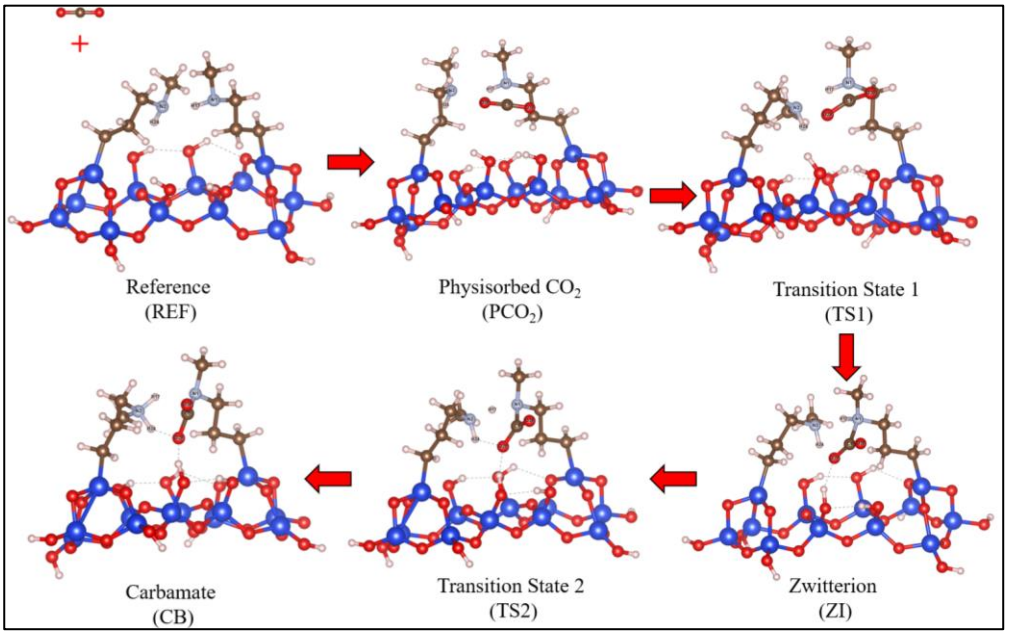

Figure 4.11. Molecular structures of the CO_2 adsorption species of the 5_4_5-MAPS ZCB mechanism

4.2.3. Isolated Carbamic Acid Formation Route (ICA)

Similar to the 5_5-MAPS, ICA mechanism involved the intramolecular formation of carbamic acid through the transfer of a proton from the CO_2-adsorbed amine to the =CO of the CO_2. Activation barrier found for this transfer was 161.2 kJ/mol, which was close to the value (155.8 kJ/mol) estimated for 5_5-MAPS. This indeed indicated that ICA mechanism was kinetically unfavorable over both models, parallel to the previous findings reported for APTMS [83,86]. Obtained carbamic acid had no hydrogen bonds and it was designated as type III. Accordingly, it was 34.2 kJ/mol less stable with respect to the REF structure demonstrating the thermodynamic infeasibility of the mechanism. Physisorption energy was calculated as 1.1 kJ/mol that was much lower than the values obtained in case of DCB and ZCB mechanisms. Schematic drawing of the ICA mechanism is given in Figure 4.6, whereas the molecular structures of the reaction species can be seen in Figure 4.12.

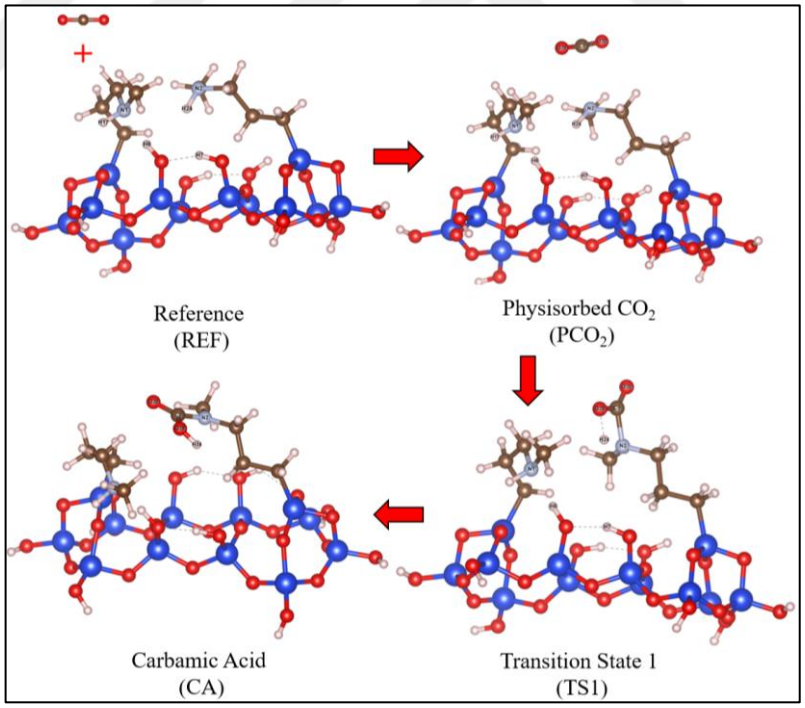

Figure 4.12. Molecular structures of the CO_2 adsorption species of the 5_4_5-MAPS ICA mechanism

4.2.4. Direct Carbamic Acid Formation Route (DCA)

In the DCA route, as it was in the 5_5-MAPS case, direct formation of carbamic acid via simultaneous proton transfer from the CO_2-adsorbed amine to the neighboring one and from this neighboring amine to the =CO of the CO_2 took place without the presence of a reaction intermediate (Figure 4.4). Physisorption energy was estimated as 14.4 kJ/mol while the activation barrier was 83.2 kJ/mol (Figure 4.8). Calculated physisorption energy was much higher than the value obtained for the DCA mechanism of 5_5-MAPS, while the activation barrier was comparable (79.8 kJ/mol in case of 5_5-MAPS). Final carbamic acid structure was of type I and was 10.1 kJ/mol more stable relative to the reference state. Molecular structures of the CO_2 adsorption species of DCA over 5_4_5-MAPS are presented in Figure 4.13.

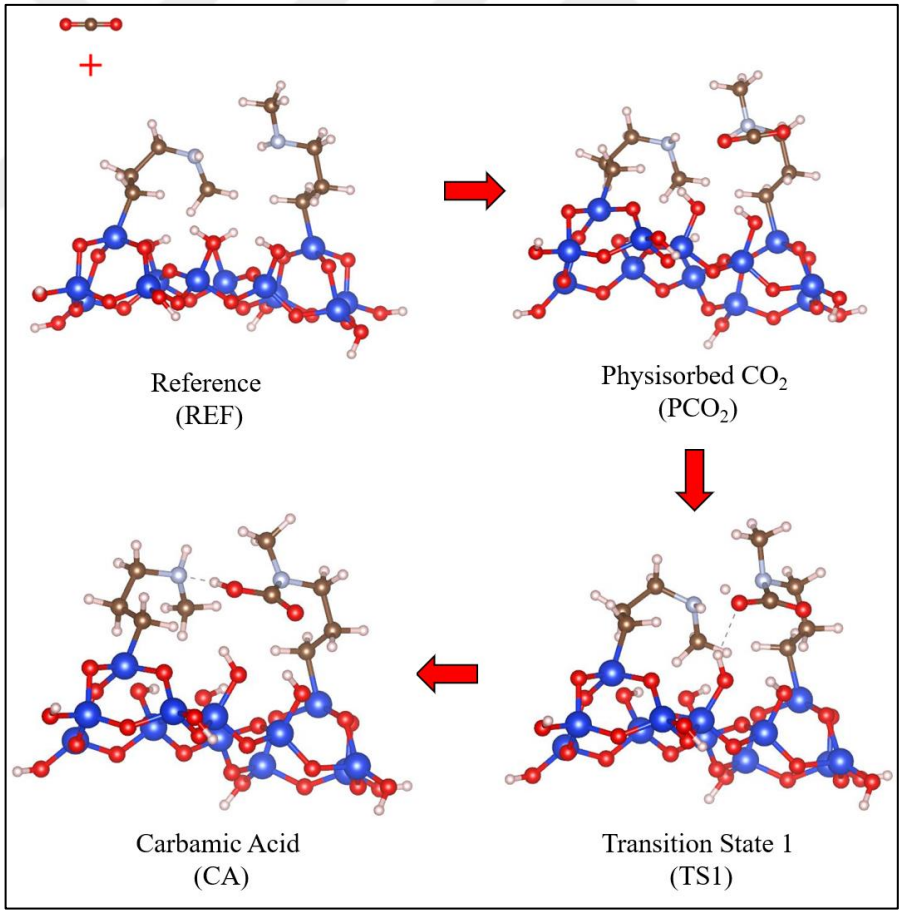

Figure 4.13. Molecular structures of the CO_2 adsorption species of the 5_4_5-MAPS DCA mechanism

4.2.5. Zwitterion to Carbamic Acid Formation Route (ZCA)

In the ZCA route, different from the DCA, carbamic acid formation took place through the evolution of the zwitterionic intermediate. According to the reaction pathway, firstly, zwitterion was created from the physisorbed CO_2 with an activation barrier of 7.1 kJ/mol. Following this, zwitterionic intermediate was deprotonated by the neighboring amine whereas a simultaneous back protonation to the =CO of the zwitterion took place with a barrier of 41.0 kJ/mol. A similar pathway was reported over 5_4_5-APTMS before, both barriers being comparable to the values reported previously (8.9 kJ/mol for the first step, 36.3 kJ/mol for the second step) [83]. Similar to the ZCB path, formation of the zwitterionic intermediate decreased the activation energy of the carbamic acid formation considerably. Calculated physisorption energy was 0.7 kJ/mol, while the zwitterion was 12.6 kJ/mol less stable than the reference point. Resulting carbamic acid was of type I and was 6.8 kJ/mol more stable relative to the reference state. The carbamic acid structure obtained in the ZCA of 5_4_5-APTMS was considerably more stable (with a relative energy of 27.6 kJ/mol compared to the reference) but this was probably stemming from the enhanced hydrogen bonding interactions rather than the functionality. Schematic drawing of the ZCA mechanism is given in Figure 4.14, whereas the molecular structures of the CO_2 adsorption species of ZCA over 5_4_5-MAPS can be seen in Figure 4.15.

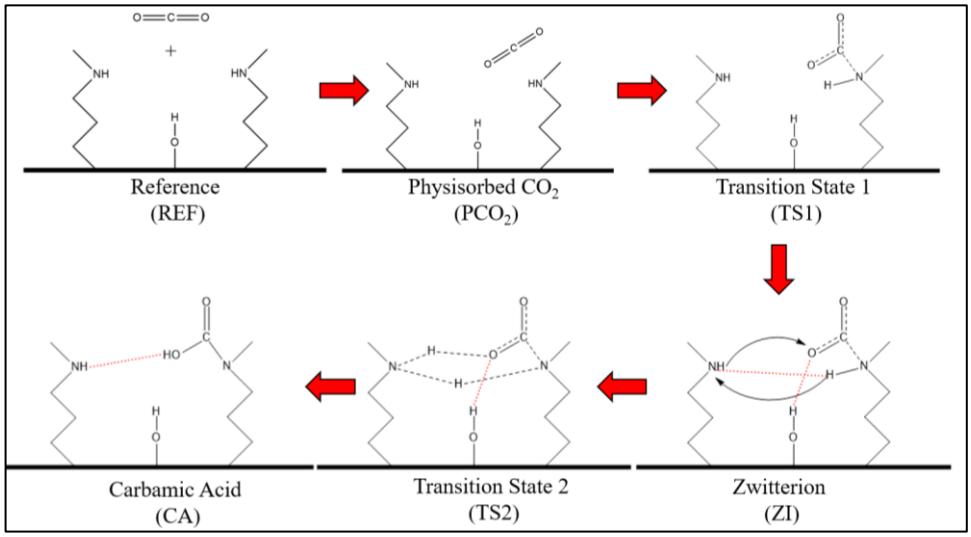

Figure 4.14. Schematic drawing of the 5_4_5-MAPS ZCA mechanism

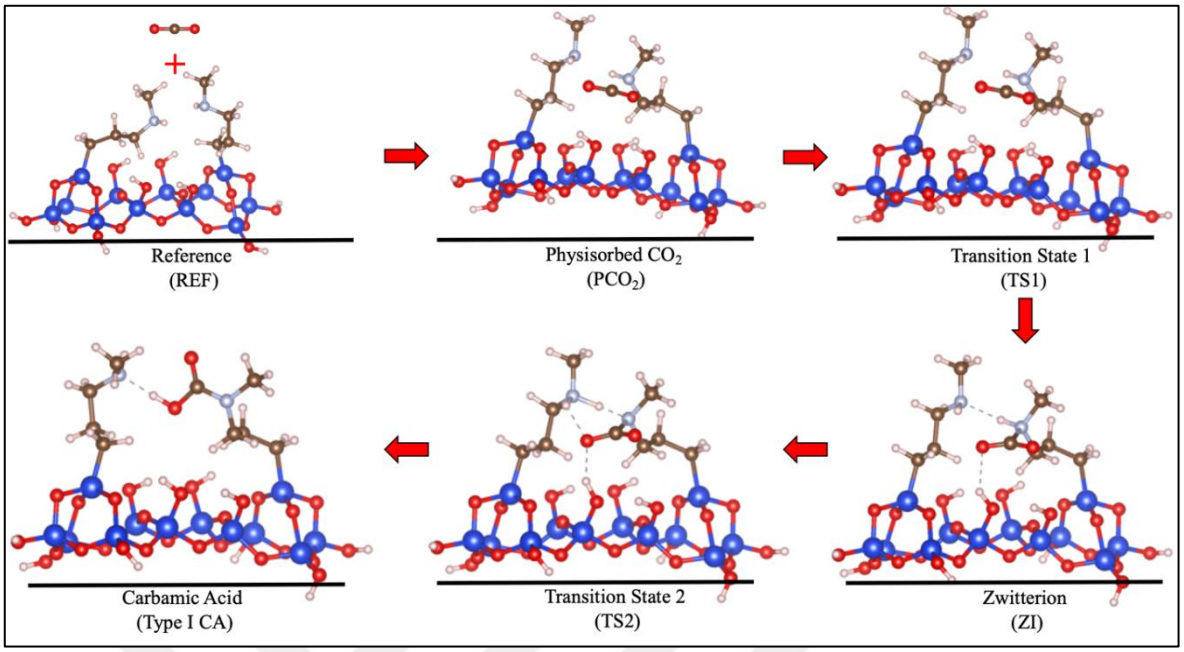

Figure 4.15. Molecular structures of the CO_2 adsorption species of the 5_4_5 MAPS ZCA mechanism

4.2.6. Carbamate to Carbamic Acid Formation Route (CBA)

In the CBA mechanism, ammonium carbamate ion pair acted as a reaction intermediate in the formation of carbamic acid. According to the observed pathway, in the first step physisorbed CO_2 (with an adsorption energy of 12.1 kJ/mol) was converted to an ammonium carbamate with an activation barrier of 69.6 kJ/mol, similar to the DCB mechanism. This structure was hydrogen bonded to one of the free silanols through its –CO and to one of the hydrogens of the ammonium through its =CO group and was found to be 4 kJ/mol more stable relative to the reference state. Following this, back protonation of the =CO group took place spontaneously (reaction barrier was -7.8 kJ/mol) resulting in the formation of a carbamic acid. Obtained structure was hydrogen bonded to the neighboring amine through its –COH group and to the surface silanol through its =CO group, and was denoted as Type II. Its relative energy was calculated as -11.8 kJ/mol with respect to the reference point. The schematic drawing of the reaction path can be seen in Figure 4.16, while the molecular structures of the adsorption species are presented in Figure 4.17.

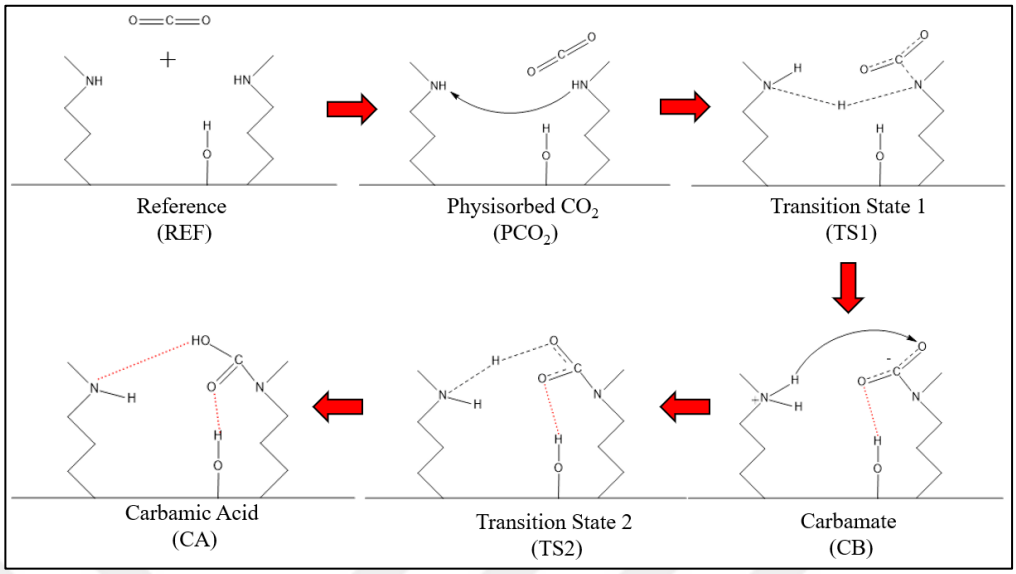

Figure 4.16. Schematic drawing of the 5_4_5-MAPS CBA mechanism

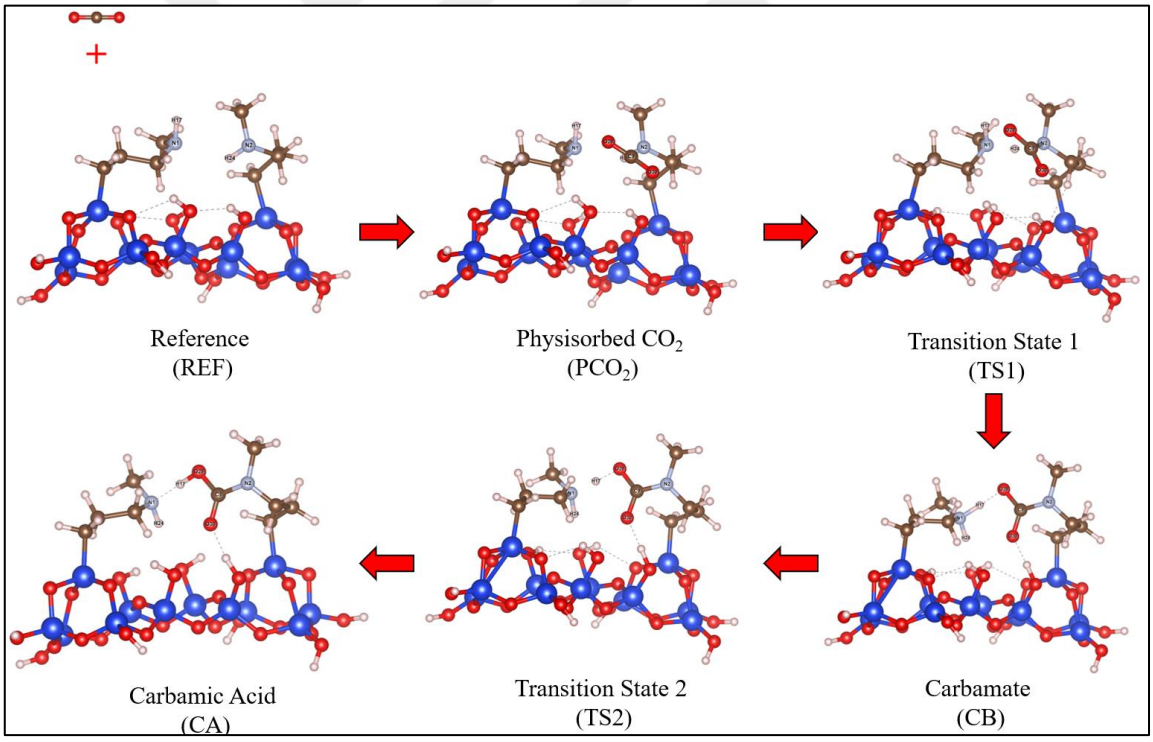

Figure 4.17. Molecular structures of the CO_2 adsorption species of the 5_4_5-MAPS CBA mechanism

4.2.7. Surface-mediated carbamate to carbamic acid formation route (SCBA)

Different from the reaction pathways discussed above, free surface silanols played an active role in the reaction mechanism in the SCBA route. According to the identified pathway (Figure 4.18), physisorbed CO_2 (adsorption energy being 1.1 kJ/mol) was transformed into an ammonium carbamate through a simultaneous proton transfer from the CO_2-adsorbed amine to the nearest -OH and from this silanol to the neighboring amine. The carbamate structure obtained in this way was hydrogen bonded to two free surface silanols through its –CO group and to the neighboring ammonium through its =CO and was calculated to be 37.1 kJ/mol more stable with respect to the reference state due to the enhanced hydrogen bonding interactions. Estimated activation barrier for this step was 129.0 kJ/mol, being considerably higher than the values calculated for the DCB (64.7 kJ/mol) and CBA (69.6 kJ/mol) mechanisms. Following this, back protonation of the =CO group by the ammonium took place with an activation energy of 2.1 kJ/mol. Resulting carbamic acid was of type II and 31.6 kJ/mol more stable than the reference. Figure 4.8 summarizes the reaction energetics of the SCBA route, while Figure 4.19 presents the molecular structures of the adsorption species.

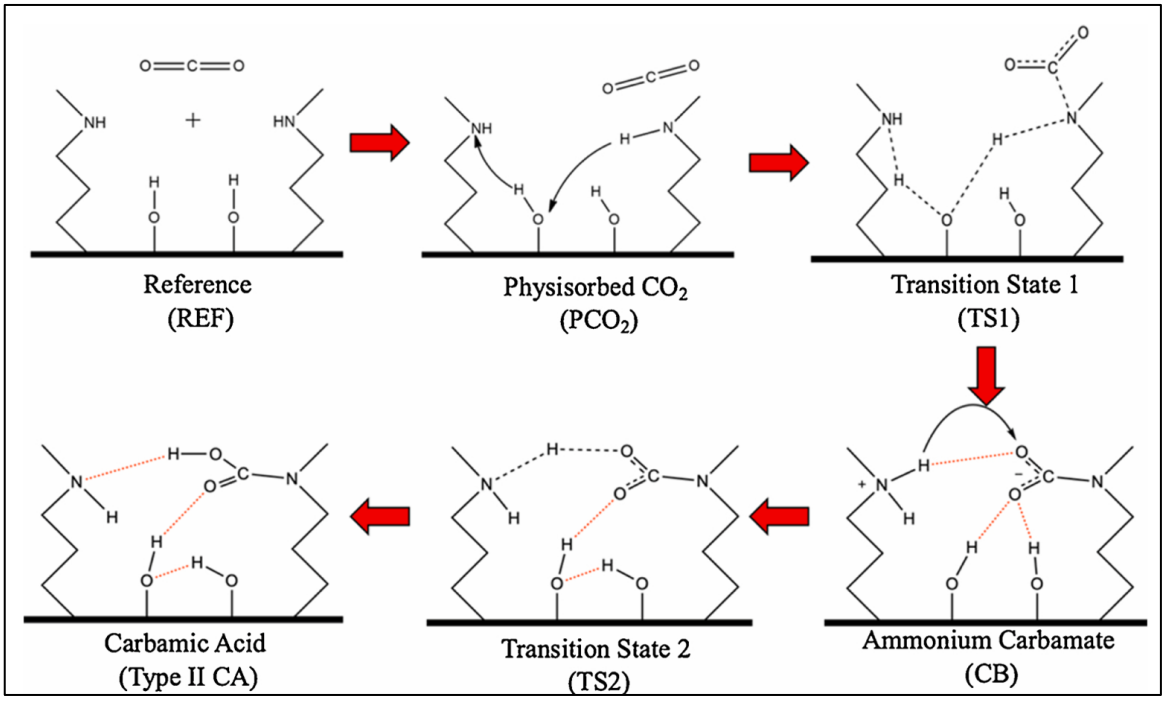

Figure 4.18. Schematic drawing of the 5_4_5-MAPS SCBA mechanism [82]

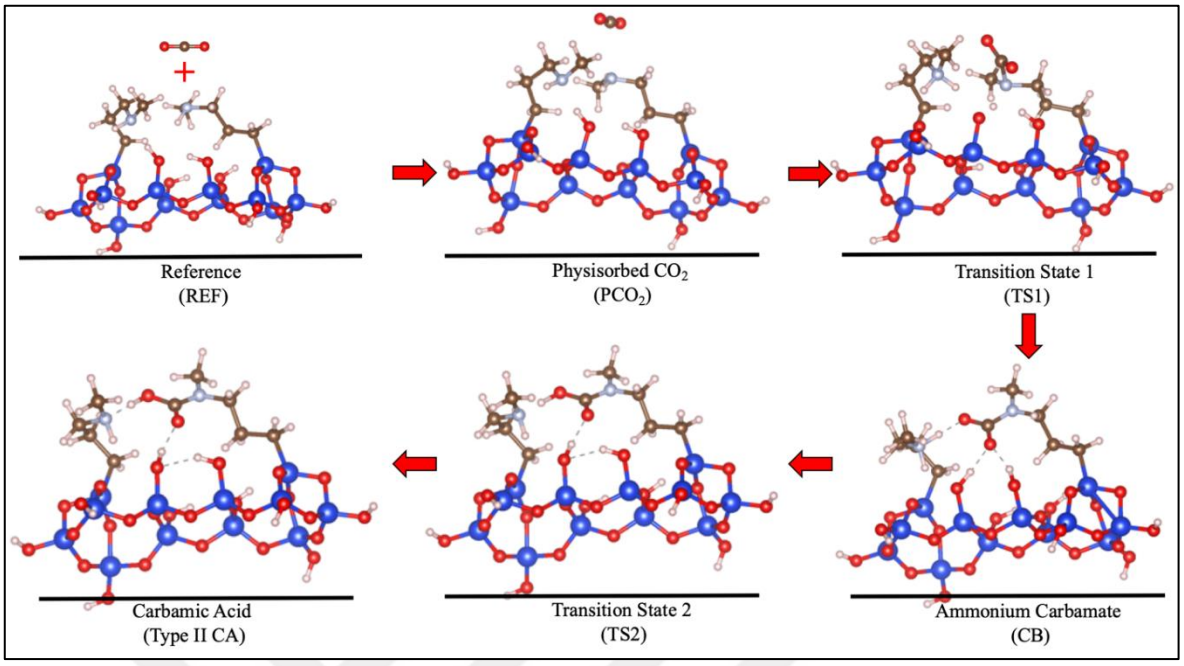

Figure 4.19. Molecular structures of the CO_2 adsorption species of the 5_4_5-MAPS SCBA mechanism

4.2.8. Surface-Mediated Carbamate to Carbamic Acid Formation through an Intermediate Route (SCBIA)

The SCBIA route was indeed quite similar to the SCBA path, the only difference being the formation of a reaction intermediate between the physisorbed CO_2 and the carbamate. Accordingly, a proton was transferred from one of the free surface silanols to the amine molecule other than the CO_2-adsorbed one in the first step forming a SiO^--NH_2^+-NHCOO complex with a reaction barrier of 42.7 kJ/mol. Following this, SiO^- was back protonated by the CO_2-adsorbed amine leading to the formation of an ammonium carbamate with a barrier of 45.6 kJ/mol. The formation of the reaction intermediate seemed to decrease the required barrier for the evolution of carbamate significantly when compared to the barrier calculated for the SCBA mechanism. Finally, in the last step carbamate was protonated by the ammonium forming the carbamic acid as the end-product and the activation barrier calculated for this step was 3.3 kJ/mol. Physisorption energy was estimated as 1.7 kJ/mol, while the relative energy of the reaction intermediate was +47.3 kJ/mol with respect to the reference. Similar to the SCBA case, carbamate was involved in a hydrogen bonding network with the surface silanols and the ammonium and accordingly was found to be

thermodynamically stable (relative energy of -32.1 kJ/mol relative to the reference state). The end-product was a carbamic acid of type II and was 25.2 kJ/mol more stable than the reference state. The schematic drawing of the mechanism is given in Figure 4.20 and the adsorption species may be seen in Figure 4.21.

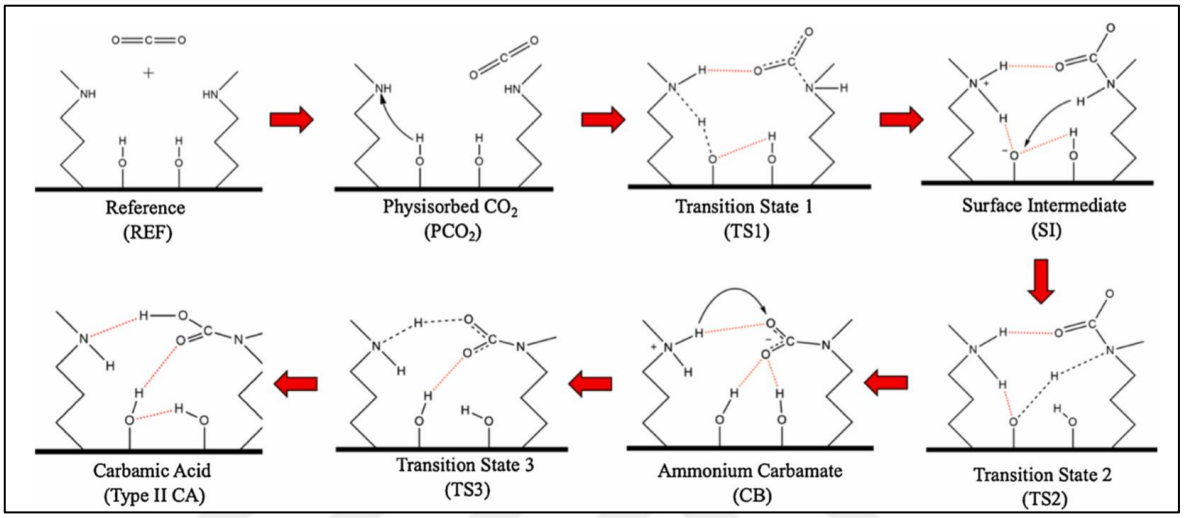

Figure 4.20. Schematic drawing of the 5_4_5-MAPS SCBIA mechanism

This mechanism was indeed very similar to the one studied for APTMS before by Cho et al. except for the absence of a zwitterionic structure between the physisorbed CO_2 and the reaction intermediate in here [68]. Their reaction energetics was given in terms of electronic energy so comparison was achieved in terms of electronic energies. Their calculated barrier for the transformation of the reaction intermediate into ammonium carbamate was 33.9 kJ/mol while ours was 50.6 kJ/mol, stemming probably from the presence of the zwitterionic intermediate. The activation barrier estimated for the transformation of carbamate into carbamic acid in this study (13. 9 kJ/mol) was, on the other hand, slightly lower than theirs (21.3 kJ/mol). When the relative stabilities of the carbamate and carbamic acid were taken into consideration, estimated energies respectively for the carbamate and carbamic acid relative to the reference were -80.4 kJ/mol and -67.1 kJ/mol in this study; -81.2 kJ/mol and 63.2 kJ/mol in their study. However, the surface bound siloxide-carbamic acid-ammonium complex reported in their study was found to be not stable under the conditions employed in our study [68].

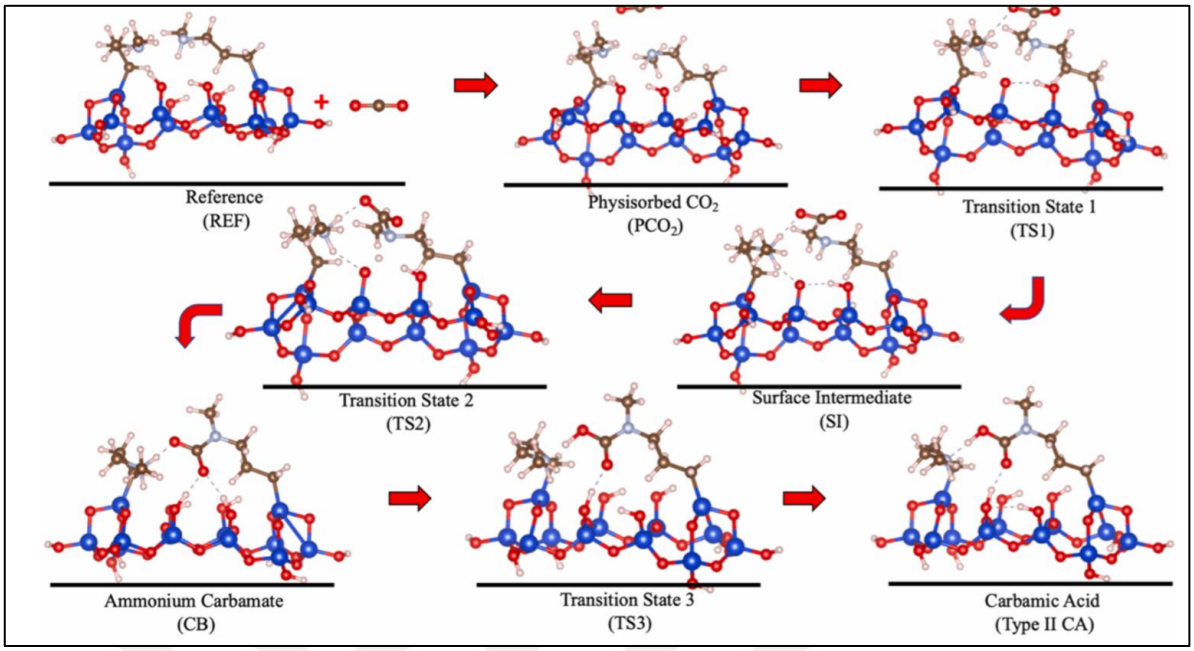

Figure 4.21. Molecular structures of the CO_2 adsorption species of the 5_4_5-MAPS SCBIA mechanism

4.2.9. Carbamate to Surface-Mediated Carbamic Acid Formation through the Zwitterion Route (ZCBSA)

The ZCBSA route (Figure 4.22), which was previously reported for 5_4_5_APTMS too [82], was identical to the ZCB mechanism until the formation of the ammonium carbamate. Accordingly, zwitterionic intermediate was formed from the physically-adsorbed CO_2 in the first step, this structure subsequently being transformed into an ammonium carbamate through the deprotonation of the zwitterion. The activation barriers calculated for these steps were 20.0 kJ/mol and 32.8 kJ/mol, respectively while the relative energies of the physisorption state, the zwitterion and the carbamate with respect to the reference were -3.1 kJ/mol, 21.0 kJ/mol, and 55.8 kJ/mol, respectively (Figure 4.8). There was then a simultaneous H transfer from the obtained ammonium to a nearby surface silanol and from this silanol to the –CO of the carbamate resulting to the formation of a carbamic acid. This step required a reaction barrier of 109.0 kJ/mol. Final carbamic acid structure was hydrogen bonded to the surface silanol through its –COH and to the neighboring amine through its =CO and was designated as type V. It was found to be 20.0 kJ/mol more stable compared to the reference state. Molecular structures of the CO_2 adsorption species may be found in

Figure 4.23. The reaction barriers calculated in this study for the second and third steps were considerably higher than those of the 5_4_5-APTMS reported previously (12.3 kJ/mol and 31.4 kJ/mol, respectively) [83].

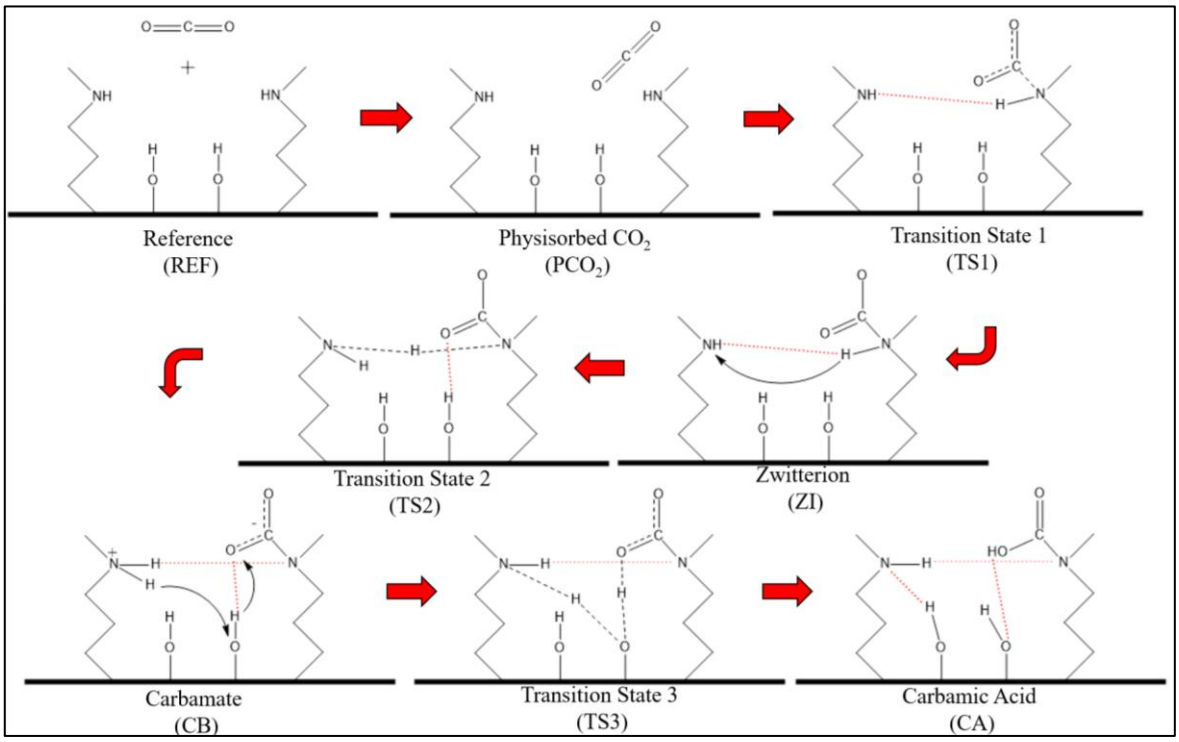

Figure 4.22. Schematic drawing of the 5_4_5-MAPS ZCBSA mechanism

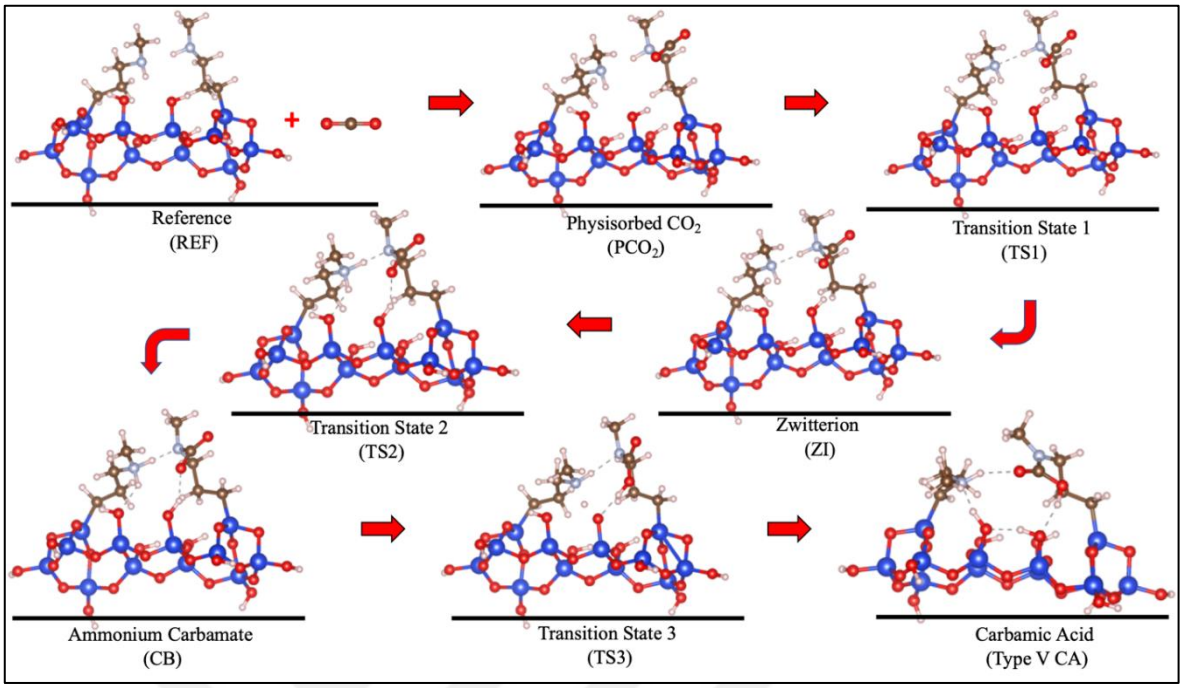

Figure 4.23. Molecular structures of the CO_2 adsorption species of the 5_4_5-MAPS ZCBSA mechanism

Reaction pathway analysis performed over 5_4_5-MAPS revealed that the interaction of the reaction species with the surface was more pronounced in comparison with 5_5-MAPS. As a result, reaction pathways including the stabilization of the zwitterionic intermediate as well as the active participation of the surface silanols in the reaction mechanism were observed. However, the steric hindrance caused by the –CH3 group bonded to the secondary amine of the MAPS molecule was still more restrictive on surface interactions relative to the previously reported 5_4_5-APTMS case [83]. Thus, the number of conformers resulting in very complex hydrogen bonding networks which was indispensable for the stabilization of reaction species were much fewer compared to the APTMS and the product stabilities as well as the activation energies were either similar to those of APTMS or much inferior in case of MAPS.

On the other hand, physisorption energies calculated over 5_4_5-MAPS were slightly higher than the values reported over 5_4_5-APTMS before [83]. The replacement of the hydrogen atom by a –CH3 group in a secondary amine was indeed reported to either increase the reactivity towards CO_2 due to the enhanced basicity or decrease the reactivity due to the

expanded steric hindrance [85]. As discussed above, the enhancement observed in the CO_2 adsorption energies over 5_4_5-MAPS compared to 5_4_5-APTMS might be stemming from the much closer orientation of CO_2 to the surface but also from the higher affinity of secondary amines towards CO_2, as demonstrated previously [4,43,65,84,87]. The latter discussion was, however, ruled out based on the previous calculations performed over unsupported APTMS and MAPS molecules [83] proving that the steric hindrance was more dominant under the conditions employed in here.

Among the mechanisms identified over 5_4_5-MAPS, SCBIA route was demonstrated to be both thermodynamically and kinetically feasible indicating that both ammonium carbamate and carbamic acid might be observed in the product stream and the surface silanols not only took part in the stabilization of the adsorption species but also participated directly in the adsorption mechanism. Besides, our calculations demonstrated that carbamate formation was thermodynamically and kinetically possible in the presence of a complex hydrogen bonding network which supported the assignment of an ionic ammonium carbamate pair to the frequently observed ^{13}C NMR resonance at ~164 ppm (species C) [83].

5. CONCLUSION AND RECOMMENDATIONS

This study was carried out to shed a light on the CO_2 adsorption mechanisms over MAPS-functionalized mesoporous silica and to determine the potential effect of the surface silanols on the reaction mechanism. Our results obtained by using two different mesoporous silica models resulting in two distinct surface amine densities and surface silanol densities were compared to the previous findings reported for APTMS as well, with the purpose of elucidating the effect of amine functionality (primary or secondary) on the CO_2 adsorption. Following conclusions can be drawn based on the calculations performed:

- Carbamic acid and ammonium carbamate were the two main products of CO_2 adsorption over MAPS-functionalized mesoporous silica.
- Formation of carbamic acid was more feasible in case of restricted surface interaction. However, if the surface interaction is available and complex hydrogen bonding networks are present, stabilities of carbamic acid and ammonium carbamate are similar.
- Formation of both carbamate and carbamic acid required the presence of amine pairs underlining the significance of the surface amine density on the CO_2 adsorption performance of the sorbents.
- Various carbamic acid structures being involved in distinct hydrogen bonding networks and having resultantly different product stabilities were identified implying that carbamic acid structures that can be found in reaction streams may differ from one another.
- Hydrogen bonding interactions were quite effective in stabilization of the adsorption species and reaction kinetics.
- Surface silanols played a significant role on the adsorption of CO_2. They not only played a critical role on the formation and stabilization of the reaction species but could also participate directly in the adsorption mechanism underlining the importance of the free surface silanol density on the CO_2 capture performance.
- Amine functionality seemed to be less decisive on the reaction kinetics and thermodynamics under the conditions employed.

Following recommendations are believed to be useful in clarification of the CO_2 capture mechanisms over amine-functionalized mesoporous silica which in turn will help to develop high-performance sorbents:

- Effect of humidity on the reaction mechanisms as well as product stabilities may be investigated
- Multi-amine-based sorbents may be examined in order to determine whether intramolecular capture is possible
- Various amines with different structural properties may be studied with the purpose of establishing a structure-activity relation between amine properties and CO_2 affinity.

REFERENCES

1. Neilsen CJ, Herrmann H, Weller C. Atmospheric chemistry and environmental impact of the use of amines in carbon capture and storage (CCS). *Chem. Soc. Rev.* 2012;41:6684-704.
2. Audus H. Greenhouse Gas mitigation technology: an overview of the CO_2 capture and sequestration studies and further activities of the IEA greenhouse gas R&D program. *Energy.* 1997;2/3:217-21.
3. Xu X, Song C, Andresen JM, Miller BG, Scaroni AW. Novel polyethylenimine-modified mesoporous molecular sieve of MCM-41 type as high-capacity adsorbent for CO_2 capture. *Energy & Fuel.* 2002;16:1463-9.
4. Zeleňák V, Badaničová M, Halamová D, Čejka J, Zukal A, Murafa N, Goerigk G. Amine-modified ordered mesoporous silica: Effect of pore size on carbon dioxide capture. *Chemical Engineering Journal.* 2008;144:336-42.
5. Zheng F, Tran DN, Busche BJ, Fryxell GE, Addleman RS, Zemanian TS, Aardahl CL. Ethylenediamine-modified SBA-15 as regenerable CO_2 sorbent. *Ind. Eng. Chem. Res.* 2005;44:3099-105.
6. Hoffmann F, Cornelius M, Morell J, Fröba M. Silica-based mesoporous organic-ınorganic hybrid materials. *Angew. Chem. Int. Ed.* 2006;45:3216-51.
7. Daryayehsalameh B, Nabavi M, Vaferi B. Modeling of CO_2 capture ability of [Bmim][BF_4] ionic liquid using connectionist samart paradigms. *Environmental Technology & Innovation.* 2021;22:101484.
8. Bains P, Psarras P, Wilcox J. CO_2 capture the industry sector. *Progress in Energy and Combustion Science.* 2017;63:146-72.
9. Lu H, Guan Y, He L, Adhikari H, Pellikka P, Heiskanen J, Maeda E. Patch aggregation trends of the global climate landscape under future global warming scenario. *Int. J. Climatol.* 2020;40:2674-85.
10. United States Environmental Protection Agency: Global Greenhouse Gas Emissions Data; [cited 2021 8 September]. Available from: https://www.epa.gov/ghgemissions/global-greenhouse-gas-emissions-data.
11. Houghton JT, Ding Y, Griggs DJ, Noguer M, Van Der Linden PJ and Xiaosu D. The Physical Science Basis. *Working Group 1 Contribution to the Third Assessment Report of the Intergovernmental Panel on Climate Change (IPCC)*;2001:IPCC.

12. Hansen J, Sato M, Kharecha P, Beerling D, Berner R, Masson-Delmotte V, Pagani M, Raymo M, Royer DL,Zachos JC. Target atmospheric CO_2: Where should humanity aim?. *Open Atmos. Sci. J.* 2008;2:217-31.
13. Jensen D, Gazzani M, Manzolini G, Dijk EV, Carbo M. Pre-combustion CO_2 capture. *International Journal of Greenhouse Gas Control.* 2015;40:167-87.
14. Davran-Candan T. CO_2 capturing materials. *Comprehensive energy systems.* 2018:881-912.
15. Fevre E. Membrane processes and postcombustion carbon dioxide capture: Challenges and prospects. *Chemical Engineering Journal.* 2011;171:782-93.
16. Handogo R. Carbon capture and storage system using pinch design method. *MATEC Web of Conferences.* 2018;156:03005.
17. Kohl, A. L.; Nielsen, R. B. Gas Purification (5th Edition); Elsevier: Houston, 1997.
18. Lepaumier H, Silva EF, Einbu A, Grimstvedt A, Knudsen JN, Zahlsen K, Svendsen HF. Comparison of MEA degradation in pilot-scale with lab-scale experiments. *Energy Procedia.* 2011;4:1652-9.
19. Davis J, Rochelle G. Thermal degradation of monoethanolamine at stripper conditions. *Energy Procedia.* 2009;1:327-33.
20. Sakwattanapong R, Aroonwilas A, Veawab A. Behavior of heat duty for CO_2 capture plants using regenerable single and blended alkanolamines. *Ind. Eng. Chem. Res.* 2005;44:4465-73.
21. Veawab A, Tontiwachwuthikul P, Chakma A. Corrosion behavior of carbon steel in the CO_2 absorption process using aqueous amine solutions. *Ind. Eng. Chem. Res.* 1999;38:3917-24.
22. Khan AA, Halder GN, Saha AK. Comparing CO_2 removal characteristics of aqueous solutions of monoethanolamine, 2-amino-2-methyl-1-propanol, methyldiethanolamine and piperazine through absorption process. *International Journal of Greenhouse Gas Control.* 2016;50:179-89.
23. Tontiwachwuthikul P, Meisen A, Lim CJ. Solubility of CO_2 in 2-amino-2methyl-1-propanol solutions. *J Chem Eng Data.* 1991;36:130-3.
24. Park SH, Lee KB, Hyun JC, Kim SH. Correlation and prediction of the solubility of carbon dioxide in aqueous alkanolamine and mixed alkanolamine solutions. *Ind Eng. Chem. Res.* 2002;41:1658-65.

25. Gray ML, Champagne KJ, Fauth D, Baltrus JP, Pennline H. Performance of immobilized tertiary amine solid sorbents for the capture of carbon dioxide. *International Journal of Greenhouse Gas Control.* 2008;2:3-8.
26. Ashraf MN, Mahmood MH, Sultan M, Miyazaki T, Khan ZM. Study of CO_2 separation from flue gases by adsorption. *International Conference on Energy, Water and Environment;*2021:ICEWE.
27. Do DD, Wang K. A new model for the description of adsorption kinetics in heterogeneous activated carbon. *Carbon.* 1998; 36(10):1539-54.
28. Berlier K, Frère M. Adsorption of CO_2 on activated carbon: Simultaneous determination of integral heat and isotherm of adsorption. *J.Chem. Eng. Data.* 1996;41:1144-8.
29. Samanta A, Zhao A, Shimizu GKH, Sarkar P, Gupta R. Post-combustion CO_2 capture using solid solvents: A review. *Ind. Eng. Chem. Res.* 2012;51:1438-63.
30. Kikkinides ES, Yang RT, Cho SH. Concentration and recovery of CO_2 from flue gas by pressure swing adsorption. *Ind. Eng. Chem. Res.* 1993;32:2714-20.
31. Chue KT, Kim JN, Yoo YJ, Cho SH, Yang RT. Comparison of activated carbon and zeolite 13X for CO_2 recovery from flue gas by pressure swing adsorption. *Ind. Eng. Chem. Res.* 1995;34:591-8.
32. Siriwardane RV, Shen MS, Fisher EP, Poston JA. Adsorption of CO_2 on molecular sieves and activated carbon. *Energy & Fuels.* 2001;15:279-84.
33. Da'na E, Silva ND, Sayari A. Adsorption of copper on amine-functionalized SBA-15 prepared by co-condensation: Kinetics properties. *Chemical Engineering Journal.* 2011;166:454-9.
34. Choudhary VR, Mayadevi S, Singh AP. Sorption isotherms of methane, ethane and carbon dioxide on NaX, NaY and Na-mordenite zeolites. *J. Chem. Soc. Faraday Trans.* 1995;91(17):2935-44.
35. Demessence A, D'Alessandro D, Foo ML, Long JR. Strong CO_2 binding in a water-stable, triazolate-bridged metal-organic framework functionalized with ethylenediamine. *J. Am. Chem. Soc.* 2009;131:8784-6.
36. Wang L, Yao M, Hu X, Hu G, Lu J, Luo M, Fan M. Amine-modified ordered mesoporous silica: The effect of pore size on CO_2 capture performance. *Applied Surface Science.* 2015;324:286-92.
37. Kamran U, Park SJ. Chemically modified carbonaceous adsorbents for enhanced CO_2 capture: A review. *Journal of Cleaner Production.* 2021;290:125776.

38. Rath D, Rana S, Parida KM. Organic amine functionalized silica based mesoporous materials: An update of syntheses and catalytic applications. *Royal Society of Chemistry.* 2014;17:25-53.
39. Hoffmann F, Fröba M. Vitalizing porous inorganic silica networks with organic functions PMOs and related hybrid materials. *Chem. Soc. Rev.* 2011;40:608-20.
40. Xu GW, Zhang CF, Qin SJ, Wang YW. Kinetics study on absorption of carbon dioxide into solutions of activated methyldiethanolamine. *Ind. Eng. Chem. Res.* 1992;31:921-7.
41. Harlick PJE, Sayari A. Applications of pre-expanded mesoporous silicas. 3. Triamine silane grafting for enhanced CO_2 adsorption. *Ind. Eng. Chem. Res.* 2006;45:3248-55.
42. Hiyoshi N, Yogo K, Yashima T. Adsorption of carbon dioxide on amine modified SBA-15 in the presence of water vapor. *Chemistry Letters.* 2004;33(5):510-1.
43. Yıldız MG, Davran Candan T, Günay ME, Yıldırım R. CO_2 capture over amine-functionalized MCM-41 and SBA-15: Exploratory analysis desion tree classification of pat data. *Journal of CO_2 Utilization.* 2019;31:27-42.
44. Deng Y, Seville JPK, Bell SD, Ingram A, Zhang H, Sweygers N, Dewil R, Baeyens J,Appels L. Reviewing fundamental CO_2 adsorption characteristics of zeolite and activated carbon by in-situ measurements with radioactively labelled CO_2. *Separation & Purification Reviews*. 2021;1542:2119-27.
45. Ma X, Wang X, Song C. "Molecular basket" sorbents for separation of CO_2 and H_2S from various gas streams. *J. Am. Chem. Soc.* 2009;131:5777-83.
46. Sanz-Perez ES, Olivares Marín M, Arencibia A, Sanz R, Calleja G, Maroto-Valer MM. CO_2 adsorption performance of amino-functionalized SBA-15 under post combustion conditions. *International Journal of Greenhouse Gas Control.* 2013;17:366-75.
47. Hiyoshi N, Yogo K, Yashimi T. Adsorption characteristics of carbon dioxide on organically functionalized SBA-15. *Microporous and Mesoporous Materials.* 2005;84:357-65.
48. Liu ZL, Teng Y, Zhang K, Cao Y, Pan WP. CO_2 adsorption properties and thermal stability of different amine-impregnated MCM-41 materials. *J. Fuel Chem. Technol.* 2013;41(4):469-76.
49. Caplow M. Kinetics of carbamate formation and breakdown. *Journal of Chemical Society.* 1968;24:6795-803.

50. Versteeg GF, Dijck LAJV, Swaaij WPMV. On the kinetics between CO_2 and alkanolamines both in aqueous and non-aqueous solutions an overview. *Chem. Eng. Comn.* 1996;144:113-58.
51. Davran Candan T. DFT Modeling of CO_2 Interaction with various aqueous amine structures. *J. Phys. Chem. A.* 2014;118:4582-90.
52. Danckwerts PV. The reaction of CO_2 with ethanolamines. *Chemical Engineering Science.* 1979;34:443-6.
53. Goodrich BF, Fuente JC, Gurkan BE, Lopez ZK, Price EA, Huang Y, Brennecke JF. Effect of water and temperature on absorption of CO_2 by amine-tethered ionic liquids. *J. Phys. Chem. B.* 2011;115:9140-50.
54. Da Silva EF, Svendsen HF. Computational chemistry study reaction, equilibrium and kinetics of chemical CO_2 absorption. *International Journal of Greenhouse Gas Control.* 2007;1:-151-7.
55. Leal O, Bolívar C, Ovalles C, García JJ, Espidel Y. Reversible adsorption of carbon dioxide amine surface-bonded silica gel. *Inorganica Chimica Acta.* 1995;240:183-9.
56. Chang ACC, Chuang SSC, Gray M, Soong Y. In-situ infrared study of CO_2 adsorption on SBA-15 grafted with γ-(aminopropyl)triethoxysilane. *Energy & Fuels*. 2003;17:468-73.
57. Khatri RA, Chuang SSC, Soong Y, Gray M. Carbon dioxide capture by diamine-grafted SBA-15: A combined fourier transform infrared and spectrometry study. *Ind. Eng. Chem. Res.* 2005;44:3702-8.
58. Khatri RA, Chuang SSC, Soong Y, Gray M. Thermal and chemical stability of regenerable solid amine sorbent for CO_2 Capture. *Energy Fuels.* 2006;20:1514-20.
59. Wang X, Schwartz V, Clark JC, Ma X, Overbury SH, Xu X, Song C. Infrared study of CO_2 sorption over "Molecular basket" sorbent consisting of polyethylenimine-modified mesoporous molecular sieve. *J. Phys. Chem. C.* 2009;113:7260-8.
60. Bacsik Z, Ahlsten, Ziadi A, Zhao G, Garcia Bennett AE, Martin Matute B, Hedin N. Mechanisms and kinetics for sorption of CO_2 on bicontinuous mesoporous silica modified with n-propylamine. *Langmuir.* 2011;27:11118-28.
61. Danon A, Stair PC, Weitz E. FTIR study of CO_2 adsorption on amine-grafted SBA-15: Elucidation of adsorbed species. *J. Phys. Chem. C.* 2011;115:11540-9.

62. Zhang X, Qin H, Zheng X, Wu W. Development of efficient amine-modified mesoporous silica SBA-15 for CO_2 capture. *Material Research Bulletin.* 2013;48:3981-6.
63. Pinto ML, Mafra L, Guil JM, Pires J, Rocha J. Adsorption and activation of CO_2 by amine-modified nanoporous materials studied by solid-state NMR and $^{13}CO_2$ adsorption. *Chem. Mater.* 2011;23:1387-95.
64. Moore JK, Sakwa-Novak MA, Chaikittisilp W, Metha AK, Conradi MS, Jones CW, Hyes SE. Characterization of mixture of CO adsorption products in hyperbranched aminosilica adsorbents by C solid-state NMR. *Environmental Science & Technology.* 2015;49(22):13684-91.
65. Mafra L, Čendak T, Schneide S, Wiper PV, Pires J, Gomes JRB, Pinto ML. The structure of chemisorbed CO_2 species in amine-functionalized mesoporous silicas studied by solid-state NMR and Computer modeling. *J.Am. Chem. Soc.* 2017;139(1):389-408.
66. Aziz B, Zhao G, Hedin N. Carbon dioxide sorbent with propylamine groups-silica functionalized with a fractional design approach. *Langmuir.* 2011;27:3822-34.
67. Cendak T, Sequeira L, Sardo M, Valente A, Pinto ML, Mafra L. Detecting Proton Transfer in CO_2 species chemisorbed on amine-modified silicas by using ^{13}C NMR chemical shift anisotropy and smart control of amine surface density. *Chem. Eur. J.* 2018;24:1-11.
68. Cho M, Park J, Yavuz CT, Jung Y. A catalytic role of surface silanol groups in CO_2 capture on the amine-anchored silica support. *Physical Chemistry Chemical Physics.* 2018;20:12149-56.
69. Topçubaşı BU. Theoretical investigation of CO_2 adsorption mechanism over (3-aminopropyl)trimethoxysilane-functionalized mesoporous silica sorbents. Master Thesis, Yeditepe University, 2019.
70. Broadbelt LJ, Snurr RQ. Application of molecular modeling in heterogeneous catalysis research. *Applied Catalysis A: General.* 2000;200:23-46.
71. Adcock SA and McCammon JA. Molecular dynamics: Survey of method for simulating the activity of proteins. *Chem. Rev.* 2006;106:1589-615.
72. Hehre WJ. Ab initio molecular orbital theory. *Molecular Orbital Theory.* 1976;9:399-406.

73. Bao G, Hu G, Liu D. Numerical solution of the kohn-sham equation by finite element methods with adaptive mesh redistribution technique. *Journal of Scientific Computing.* 2013;55:372-91.
74. Q-Chem: Introduction to basis sets; [cited 2021 21 November]. Available from: https://manual.q-chem.com/5.3/Ch8.S1.html
75. Aziz B, Hedin N, Bacsik Z. Quantification of chemisorption and physisorption of carbon dioxide on porous silica modified by propylamines: Effect of amine density. *Microporous Mesoporous Materials.* 2012;159:42-9.
76. Foo GS, Lee JJ, Chen CH, Hayes SE, Sievers C, Jones CW. Elucidation of Surface Species through in situ FTIR spectroscopy of carbon dioxide adsorption on amine-grafted SBA-15. *Chem Sus Chem.* 2017;10:266-76.
77. Gatti G, Costenaro D, Vittoni C, Paul G, Crocellá V, Mangano E, Brandani S, Bordiga S, Cossi M, Marchese L, Bisio C. CO_2 adsorption on different organo-modified SBA-15 silica: A multidisciplinary study on the effects of basic surface groups. *Phys. Chem. Chem. Phys.* 2017;19:14114-28.
78. Hanwell MD, Curtis DE, Lonie DC, Vandermeersch T, Zurek E, Hutchison GR. Avogadro:An advanced semantic chemical editor, visualization, and analysis platform. J. Cheminformatics 2012;4:17.
79. Frisch MJ, Trucks GW, Schlegel HB, Scuseria GE, Robb MA, Cheeseman JR, et al Gaussian 16. Wallingford CT: Gaussian Inc; 2016
80. Becke AD. Density-Functional Thermochemistry. III. the role of exact exchange. Journal of Chemical Physics. 1993;98:5648-52.
81. Leach RA. Molecular Modelling Principles and Applications. London: Prentice Hall; 2001.
82. Grimme S, Antony J, Ehrlich S, Krieg H. A consistent and accurate ab initio parametrization of density functional dispersion correction (DFT-D) for the 94 elements H-Pu. *The Journal of Chemical Physics.* 2010;132:154104.
83. Başaran K, Topçubaşı BU, Davran-Candan T. Theoretical investigation of CO_2 adsorption mechanism over amine-functionalized mesoporous silica. *Journal of CO2 Utilization.* 2021;47:101492.
84. Mafra L, Čendak T, Schneider S, Wiper PV, Pires J, Gomes JRB, Pinto ML. Amine functionalized porous silica for CO_2/CH_4 separation by adsorption: which amine and why. *Chemical Engineering Journal.* 2018;336:612-21.

85. Yamada H, Chowdhury FA, Fujiki J, Yogo K. Enhancement mechanism of the CO_2 adsorption-desorption efficiency of silica-supported tetraethylenepentamine by chemical modification of amino groups. *ASC Sustainable Chem. Eng.* 2019;7:9574-1.
86. Didas SA, Zhu R, Brunelli NA, Sholl DS, Jones CW. Thermal, oxidative and CO_2 induced degradation of primary amines used for CO_2 capture: Effect of alkyl linker on stability. *J. Phys. Chem.* 2014;118:12302-11.
87. Sayari A, Belmabkhout Y, Da'na E. CO_2 deactivation of supported amines: Does the nature of amine matter? *Langmuir.* 2012;28:4241-7.